6 Crystal-Field Theory, Tight-Binding Method and Jahn-Teller Effect

Eva Pavarini
Institute for Advanced Simulation
Forschungszentrum Jülich GmbH

Contents

E. Pavarini, E. Koch, F. Anders, and M. Jarrell
Correlated Electrons: From Models to Materials
Modeling and Simulation Vol. 2
Forschungszentrum Jülich, 2012, ISBN 978-3-89336-796-2
http://www.cond-mat.de/events/correl12

1 Introduction

The central equation of solid-state physics is the eigenvalue problem $\hat{H}\Psi = E\Psi$, defined (in the non-relativistic limit) by the many-body Hamiltonian

$$\hat{H} = -\frac{1}{2}\sum_i \nabla_i^2 + \frac{1}{2}\sum_{i\neq i'} \frac{1}{|\boldsymbol{r}_i - \boldsymbol{r}_{i'}|} - \sum_{i,\alpha} \frac{Z_\alpha}{|\boldsymbol{r}_i - \boldsymbol{R}_\alpha|} - \sum_\alpha \frac{1}{2M_\alpha}\nabla_\alpha^2 + \frac{1}{2}\sum_{\alpha\neq\alpha'} \frac{Z_\alpha Z_{\alpha'}}{|\boldsymbol{R}_\alpha - \boldsymbol{R}_{\alpha'}|},$$

where $\{\boldsymbol{r}_i\}$ are the coordinates of the N_e electrons, $\{\boldsymbol{R}_\alpha\}$ those of the N_n nuclei, Z_α the atomic numbers, and M_α the nuclear masses.[1] The Born-Oppenheimer Ansatz

$$\Psi(\{\boldsymbol{r}_i\},\{\boldsymbol{R}_\alpha\}) = \psi(\{\boldsymbol{r}_i\};\{\boldsymbol{R}_\alpha\})\Phi(\{\boldsymbol{R}_\alpha\}), \tag{1}$$

splits the Schrödinger equation $\hat{H}\Psi = E\Psi$ into the system

$$\begin{cases} \hat{H}_e\psi(\{\boldsymbol{r}_i\};\{\boldsymbol{R}_\alpha\}) &= \varepsilon(\{\boldsymbol{R}_\alpha\})\psi(\{\boldsymbol{r}_i\};\{\boldsymbol{R}_\alpha\}), \\ \\ \hat{H}_n\Phi(\{\boldsymbol{R}_\alpha\}) &= E\Phi(\{\boldsymbol{R}_\alpha\}), \end{cases} \tag{2}$$

where the Hamilton operator for the electrons ($\hat{H}_e$) and that for the lattice ($\hat{H}_n$) are

$$\begin{aligned} \hat{H}_e &= -\frac{1}{2}\sum_i \nabla_i^2 + \frac{1}{2}\sum_{i\neq i'} \frac{1}{|\boldsymbol{r}_i - \boldsymbol{r}_{i'}|} - \sum_{i,\alpha} \frac{Z_\alpha}{|\boldsymbol{r}_i - \boldsymbol{R}_\alpha|} + \frac{1}{2}\sum_{\alpha\neq\alpha'} \frac{Z_\alpha Z_{\alpha'}}{|\boldsymbol{R}_\alpha - \boldsymbol{R}_{\alpha'}|} \\ &= \hat{T}_e + \hat{V}_{ee} + \hat{V}_{en} + \hat{V}_{nn}, \end{aligned} \tag{3}$$

$$\begin{aligned} \hat{H}_n &= -\sum_\alpha \frac{1}{2M_\alpha}\nabla_\alpha^2 + \varepsilon(\{\boldsymbol{R}_\alpha\}) \\ &= \hat{T}_n + \hat{U}_n, \end{aligned} \tag{4}$$

and where in (4) we neglect non-adiabatic corrections.[2] The electronic eigenvalue $\varepsilon(\{\boldsymbol{R}_\alpha\})$ acts as potential for the nuclei and defines a Born-Oppenheimer energy surface. While (3) describes the electronic structure, (4) yields the equilibrium crystal structure of the system and the phonon modes. If the equilibrium structure $\{\boldsymbol{R}_\alpha^0\}$ is known, for example experimentally, we can focus on (3). Because $\hat{V}_{ee}$ is not separable, with increasing N_e, finding the eigenvalues and eigenvectors of (3) becomes quickly an unfeasible task, even for a single atom. The modern approach to such many-body problems consists in building, starting from (3), minimal but material specific low-energy many-body models, which retain the essential physics of the phenomenon we want to understand [1].

The first step in model building consists in performing density-functional theory (DFT) calculations. DFT is based on the Hohenberg-Kohn theorem, which states that the ground-state energy of the many-body Hamiltonian (3) is a functional $E[n]$ of the electron density, minimized by

[1] In this lecture we use atomic units (see Appendix A).

[2] The neglected term is $\hat{\Lambda}_n = -\sum_\alpha \frac{1}{M_\alpha}\left[\frac{1}{2}\langle\psi|\nabla_\alpha^2\psi\rangle + \langle\psi|\nabla_\alpha\psi\rangle\cdot\nabla_\alpha\right]$.

the ground-state density. In the Kohn-Sham DFT scheme, the ground-state energy of (3) can be obtained by solving an auxiliary Schrödinger equation $\hat{h}_e\psi = \varepsilon\psi$, with

$$\hat{h}_e = \sum_i \left[-\frac{1}{2}\nabla_i^2 + v_R(\boldsymbol{r}_i)\right] = \sum_i \hat{h}_e(\boldsymbol{r}_i). \tag{5}$$

The auxiliary Hamiltonian describes N_e non-interacting electrons in an external potential, $v_R(\boldsymbol{r})$, chosen such that the ground-state electron density $n_0(\boldsymbol{r})$ of the auxiliary model equals $n(\boldsymbol{r})$, the ground-state electron density of the original interacting system. This potential can be written as

$$v_R(\boldsymbol{r}) = -\sum_\alpha \frac{Z_\alpha}{|\boldsymbol{r}-\boldsymbol{R}_\alpha|} + \int d\boldsymbol{r}' \frac{n(\boldsymbol{r}')}{|\boldsymbol{r}-\boldsymbol{r}'|} + \frac{\delta E_{\rm xc}[n]}{\delta n} = v_{en}(\boldsymbol{r}) + v_H(\boldsymbol{r}) + v_{xc}(\boldsymbol{r}), \tag{6}$$

where $v_H(\boldsymbol{r})$ is the long-range Hartree term and $E_{\rm xc}[n]$ is the so-called exchange-correlation functional. The main difficulty of DFT is that $E_{\rm xc}[n]$ is not know, and it is therefore necessary to find good approximations for it. Most common are the local-density approximation (LDA) and its extensions; they work remarkably well for several classes of materials and properties, as discussed in the lecture of David Singh. The class of systems at the center of this school, however, is made of compounds for which many-body effects *beyond* the LDA play a crucial role, leading to cooperative emergent phenomena; examples are transition-metal oxides with partially filled d-shells, Mott insulators, Kondo systems, and heavy fermions. For such *strongly correlated materials* simple approximations to $E_{\rm xc}[n]$ fail, even qualitatively.

For strongly correlated systems, the second step consists in using DFT to construct a *localized* one-electron basis; this is usually achieved building from the Bloch functions $\psi_{n\boldsymbol{k}\sigma}(\boldsymbol{r})$, obtained by solving (5) for a given crystal, material-specific Wannier functions

$$\psi_{in\sigma}(\boldsymbol{r}) = \frac{1}{\sqrt{N}} \sum_{\boldsymbol{k}} e^{-i\boldsymbol{R}_i\cdot\boldsymbol{k}}\, \psi_{n\boldsymbol{k}\sigma}(\boldsymbol{r}).$$

Localized Wannier functions can be constructed using different procedures: the downfolding approach, discussed in [2] and in the lecture of Ole Andersen, the maximally-localized Wannier functions algorithm of Marzari and Vanderbilt [3], and the projectors technique, described in the lecture of Sasha Lichtenstein.

The third step consists in writing the Hamiltonian (3) in second quantization using such localized Wannier functions as one-electron basis. The resulting many-body Hamiltonian is the sum of an LDA term $\hat{H}^{\rm LDA}$, a Coulomb term $\hat{U}$, and a double-counting correction $\hat{H}_{\rm DC}$

$$\hat{H}_e = \hat{H}^{\rm LDA} + \hat{U} - \hat{H}_{\rm DC}. \tag{7}$$

The LDA part of the Hamiltonian is given by

$$\hat{H}^{\rm LDA} = -\sum_\sigma \sum_{in,i'n'} t_{n,n'}^{i,i'} c_{in\sigma}^\dagger c_{i'n'\sigma}, \tag{8}$$

where $c_{in\sigma}^\dagger$ ($c_{in\sigma}$) creates (annihilates) an electron of spin σ in orbital n at site i, and

$$t_{n,n'}^{i,i'} = -\int d\boldsymbol{r}\, \overline{\psi}_{in\sigma}(\boldsymbol{r})[-\frac{1}{2}\nabla^2 + v_{\rm R}(\boldsymbol{r})]\psi_{i'n'\sigma}(\boldsymbol{r}). \tag{9}$$

The $i \neq i'$ contributions are the hopping integrals, while the on-site ($i = i'$) term yields the crystal-field matrix

$$\varepsilon^{i,i}_{n,n'} = -t^{i,i}_{n,n'} = \int d\boldsymbol{r}\, \overline{\psi}_{in\sigma}(\boldsymbol{r}) \left[-\frac{1}{2}\nabla^2 + v_{\rm R}(\boldsymbol{r}) \right] \psi_{in'\sigma}(\boldsymbol{r}). \tag{10}$$

The Coulomb interaction $\hat{U}$ is given by

$$\hat{U} = \frac{1}{2} \sum_{ii'jj'} \sum_{\sigma\sigma'} \sum_{nn'pp'} U^{ij\, i'j'}_{np\, n'p'} c^\dagger_{in\sigma} c^\dagger_{jp\sigma'} c_{j'p'\sigma'} c_{i'n'\sigma},$$

with

$$U^{iji'j'}_{np\, n'p'} = \int d\boldsymbol{r}_1 \int d\boldsymbol{r}_2\, \frac{\overline{\psi}_{in\sigma}(\boldsymbol{r}_1) \overline{\psi}_{jp\sigma'}(\boldsymbol{r}_2) \psi_{j'p'\sigma'}(\boldsymbol{r}_2) \psi_{i'n'\sigma}(\boldsymbol{r}_1)}{|\boldsymbol{r}_1 - \boldsymbol{r}_2|}. \tag{11}$$

The Coulomb tensor (11) is discussed in [4] and in the lecture of Robert Eder. The double counting term $\hat{H}_{\rm DC}$ cancels the part of the electron-electron interaction contained and already well accounted for in $\hat{H}^{\rm LDA}$, such as the mean-field part of the exchange-correlation interaction and the long-range Hartree term; the difference $\hat{U} - \hat{H}_{\rm DC}$ is therefore a short-range many-body correction to the LDA [4]. The Hamiltonian (7) still describes the full many-body problem and further approximations are necessary to make progress. Typically electrons are divided into two types, correlated or heavy electrons (e.g., d or f open shells) and uncorrelated or light electrons. For the correlated electrons the LDA fails qualitatively, and $\hat{U} - \hat{H}_{\rm DC}$ has to be accounted for explicitly; for the light electrons we can instead assume that LDA is overall a good approximations and no correction $\hat{U} - \hat{H}_{\rm DC}$ is needed. The main effect of the light electrons is assumed to be a renormalization of the Coulomb parameters (*screening*), which, as a consequence, cannot be calculated any more as in (11); since the exact screening is not known, approximated schemes such as the constrained LDA or the constrained random-phase approximation are commonly used. These schemes are discussed in the lecture of Olle Gunnarsson. The separation of electron in light and heavy is the most delicate aspect of model building, as only in few cases the distinction is really clear cut. In most cases we can only make a reasonable guess, that has to be tested *a posteriori*, e.g., comparing with experiments, or better, when doable, extending the basis of heavy electrons to include, e.g., other states close to the Fermi level.

In the last step, the minimal material-specific many-body model is solved using many-body methods. If we solve it with the dynamical mean-field theory (DMFT) approach, the procedure described above defines the LDA+DMFT method [4].

While strong-correlation effects arise from the Coulomb matrix (11), chemistry enters mostly through the hopping integrals (9) and the crystal-field matrix (10). The purpose of this lecture is to explain the physical origin of these parameters, and the role they can play. To do this we will use some basic results of group theory. For simplicity, in most derivations we will use atomic hydrogen-like orbitals as a basis; the generalization to Wannier functions is straightforward.

The lecture is organized as follows. In section 2 we introduce group theory; we discuss the case of a free atom and the covering operations of molecules and crystals. In section 3 we analyze

how and why, in a crystal or a molecule, the atomic l-shells split, becoming the crystal-field levels; we focus in particular on the splitting due to the electric field generated at a given site by the surrounding ions. In section 4 we discuss covalency effects, which lead to the formations of bonds and bands (hopping integrals), and contribute to the splitting of atomic levels. In the last section we analyze the Jahn-Teller effect, a cooperative distortion driven by the coupling between electrons and lattice, which leads to further crystal-field splitting.

2 Elements of group theory

A *group*[3] G is a set of elements $\{g_i\}$ plus an operation, $\star$, which satisfy the following conditions

1. G is closed under group multiplication, i.e., $g_i \star g_j = g_k \in G \ \forall g_i,\ g_j \in G$
2. the *associative law* holds, i.e., $g_i \star (g_j \star g_k) = (g_i \star g_j) \star g_k \ \forall g_i,\ g_j,\ g_k \in G$
3. there is an *identity element* $e \in G$, such that $g_i \star e = e \star g_i = g_i \, \forall g_i \in G$
4. there is an *inverse element* $g_i^{-1} \in G$ to each $g_i \in G$, such that $g_i \star g_i^{-1} = g_i^{-1} \star g_i = e$

If the operation $\star$ is commutative, so that $g_i \star g_j = g_j \star g_i \ \forall g_i,\ g_j \in G$, the group is called *Abelian*. Groups with a finite number h of elements are called *finite groups*, and h is said to be the *order* of the group. An element g_i in group G is said to be *conjugated* to g_j if

$$g_i = g_X \star g_j \star g_X^{-1},$$

where g_X is some element of G. The elements of G can be collected into *classes* $\mathcal{C}_k$, each of which is made of all N_k mutually conjugated elements. The identity forms a class by itself. A *subgroup* of G is a set of elements of G which forms a group with the same multiplication operation of G, $\star$. Every group has at least two trivial subgroups, the group itself and a group formed by the identity only. A subgroup N of G is *invariant* if $gNg^{-1} = N \ \forall g \in G$.
Two groups G and G' are *homomorphic* if there is a correspondence $g_i \rightarrow g_i{}'$ between the elements of the two groups, so that

$$(g_i \star g_j)' = g_i' \star' g_j' \qquad \forall g_i, g_j \in G,$$

where $\star$ and $\star'$ are the multiplication operations of G and G', respectively. A homomorphism is in general a many-to-one correspondence, $\{g_1, g_2, \dots\} \rightarrow g_i'$. The identity of G, e, has as image the identity of G', e'; however in general there are several elements of G, $\{a_1 = e, a_2, \dots a_e\}$ which have e' as image in G'. Furthermore, if $g_j \in G$ has the image $g_j' \in G'$, all elements $\{g_j a_i\}$ have the same image g_j' in G'. The set $\{a_1, a_2, \dots a_e\}$ forms an invariant subgroup of G. If the correspondence between the elements of G' and G is one-to-one, G and G' are said to be *isomorphic*. A finite group is specified by the *multiplication table* of its elements; two groups with the same multiplication table are isomorphic.

[3] This section is a short summary of results relevant for the topics treated; it does not aim to be a rigorous introduction to group theory. For the latter, we refer the interested reader to specialized books [5, 6].

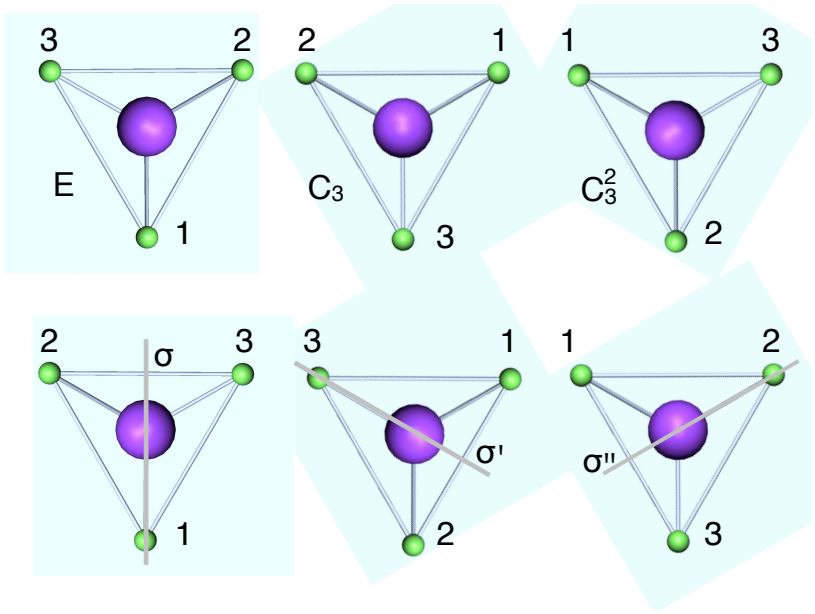

Fig. 1: *The symmetry operations which transform the ammonia molecule NH_3 into itself (viewed from the top). The point group is C_{3v}, the group of covering operations of a trigonal pyramid.*

Some of the groups relevant in physics are:

- $S(n)$, the group of permutations of n objects; $\star$ is the composition of permutations
- the group of vectors in three dimensions; $\star$ is the sum of vectors
- groups of matrices, with the matrix product as $\star$; in particular
  - $U(n)$, the group of unitary $n \times n$ matrices
  - $O(n)$, the group of orthogonal $n \times n$ matrices
  - $SU(n)$, the group of unitary $n \times n$ matrices with determinant 1
  - $SO(n)$, the group of orthogonal $n \times n$ matrices with determinant 1
  - finite groups of matrices

The group of all proper rotations in three dimensions is isomorphic to $SO(3)$. Every finite group of order n is isomorphic to a subgroup of $S(n)$. The set of all geometric symmetries that leave at least one point fixed (the origin) forms the *point group*. The point groups of crystals or molecules are isomorphic to finite subgroups of the orthogonal group $O(3)$; they are also the groups of covering operations of a given polyhedron. For example, the point group of the ammonia molecule NH_3 is the group of covering operations of a trigonal pyramid, and has six elements, shown in Fig. 1: the identity E, two rotations, by $2\pi/3$ and $4\pi/3$ (operations C_3 and $C_3^2 = C_3 \otimes C_3$), and three reflections (σ, σ', σ''). This group, called C_{3v}, has three classes, $\mathcal{C}_1 = \{E\}$, $\mathcal{C}_2 = \{C_3, C_3^2\}$, and $\mathcal{C}_3 = \{\sigma, \sigma', \sigma''\}$.

A *representation* of an abstract group G is any group G' homomorphic (or isomorphic) to G that is composed of specific operators acting on a given linear space $\mathcal{L}$. If G and G' are isomorphic the representation is said to be *faithful*. In this lecture we work with representations made of square matrices, which we indicate as $\Gamma(g_i)$; the multiplication operation of the group, $\star$, is the matrix product. As an example, we consider the group G of the rotations about the z axis. In this example, G is the abstract group. We can associate to each counterclockwise rotation by an angle θ (i.e., to each element $g = R(\theta)$ of G) a matrix $M(\theta)$

$$g = R(\theta) \rightarrow M(\theta) = \begin{pmatrix} \cos\theta & -\sin\theta \\ \sin\theta & \cos\theta \end{pmatrix}.$$

The elements of the matrix are the coefficients of the transformation

$$\begin{aligned} x' &= x\cos\theta - y\sin\theta, \\ y' &= y\sin\theta + x\cos\theta. \end{aligned}$$

The matrices $M(\theta)$ form a representation of G acting on the two-dimensional linear space $\mathcal{L}$ of vectors in the xy plane. The number of rows and columns of the matrices yields the *dimensionality* d of the representation; in the example just discussed $d = 2$.
A matrix representation Γ is called *reducible* if every matrix in the representation, $\Gamma(g_i)$, can be written in the same block form through the same *similarity transformation*.[4] If this cannot be done, the representation is said to be *irreducible*. For example if

$$\Gamma(g_i) = \begin{pmatrix} \Gamma_1(g_i) & 0 \\ 0 & \Gamma_2(g_i) \end{pmatrix} \quad \forall g_i \in G,$$

the representation Γ is said to be reducible. The number of irreducible representations is equal to the number of the classes. If the group is Abelian, the number of irreducible representations equals the number of elements and the irreducible representations are all one dimensional.
If the matrices of a representation are unitary, the representation is said to be *unitary*. A representation of a finite group made of non-singular $n \times n$ matrices is equivalent, through a similarity transformation, to a representation by unitary matrices. For finite groups, it is therefore always possible to work with unitary representations. There is nevertheless an infinite number of equivalent representations of a group G, and thus a large arbitrariness in the form of the representation. However the trace of a matrix is invariant under a similarity transformation; it is therefore useful to classify matrix representations through their *characters*, defined as

$$\chi(g_i) = \mathrm{Tr}\ \Gamma(g_i).$$

The matrix representations of all the elements g_k in a given class, $\mathcal{C}_k$, have the same character, $\chi(g_k) = \chi(\mathcal{C}_k)$, $\forall g_k \in \mathcal{C}_k$. Furthermore the following *orthogonality relations* hold for the

[4] A similarity transformation is the transformation of a $n \times n$ matrix Γ into another $n \times n$ matrix $\Gamma' = B^{-1}AB$, where B is an invertible $n \times n$ matrix.

irreducible representations Γ_j of a given group

$$\sum_i [\chi_{j_1}(g_i)]^* \chi_{j_2}(g_i) = \sum_k N_k [\chi_{j_1}(\mathcal{C}_k)]^* \chi_{j_2}(\mathcal{C}_k) = h\delta_{j_1,j_2}, \tag{12}$$

$$\sum_j [\chi_j(\mathcal{C}_k)]^* \chi_j(\mathcal{C}_l) = \frac{h}{N_k}\delta_{l,k}, \tag{13}$$

where $h = \sum_k N_k$ is the order of the group, N_k the number of elements in the class, and where for simplicity we have assumed that the irreducible representations are unitary matrices.
It is convenient to display the characters of irreducible representations in a *character table*. For the point group C_{3v} such character table is

C_{3v}	E	$2C_3$	$3\sigma_v$
Γ_1	1	1	1
Γ_2	1	1	-1
Γ_3	2	-1	0

where for each class a representative element and, in front of it, the number of elements in the class, N_k, are given (here $\mathcal{C}_1 \to E$, $\mathcal{C}_2 \to 2C_3$, $\mathcal{C}_3 \to 3\sigma_v$). The orthogonality relations tell us that different columns or different rows (the latter with weights N_k, see (12)) form orthogonal vectors. The first column of the character table is the trace of the identity and therefore yields the dimensionality of the irreducible representation. The first irreducible representation, Γ_1, has character 1 for every element of the group, and it is called *trivial representation*. The trivial representation exists for any group and is one dimensional. If an object (a molecule or a crystal) is invariant under all symmetry operations of a given group, we can say that it transforms according to the trivial representation.
A reducible representation can be decomposed in irreducible ones using the orthogonality relations of characters. One can show that, if $\chi(g_i)$ are the characters of the reducible representation, they must be given by a linear combination of the characters of irreducible representations

$$\chi(g_i) = \sum_j a_j \chi_j(g_i),$$

where the coefficients are determined from the orthogonality relations

$$a_j = \frac{1}{h}\sum_k N_k [\chi_j(\mathcal{C}_k)]^* \chi(\mathcal{C}_k).$$

Hence

$$\Gamma = a_1\Gamma_1 \oplus a_2\Gamma_2 \oplus \cdots = \bigoplus_j a_j \Gamma_j. \tag{14}$$

In quantum mechanics we are interested in the group of symmetry operators $O(g)$ which leave the Hamiltonian invariant, the *group of the Hamiltonian*, and in their action on wavefunctions. It is therefore important to know how a symmetry operator acts on a function $f(\boldsymbol{r})$ and on an operator $\hat{H}$. A function $f(\boldsymbol{r})$ is transformed by the symmetry operation $O(g)$ into the function

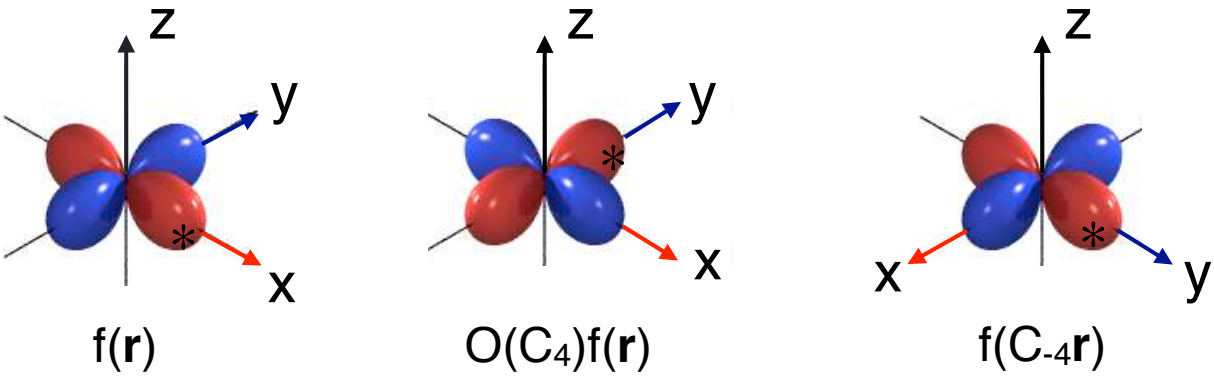

Fig. 2: *Rotation of an $x^2 - y^2$ atomic orbital by an angle $2\pi/4$ about the z axis (operation C_4).*

$O(g)f(\boldsymbol{r}) = f'(\boldsymbol{r}')$, where $\boldsymbol{r}' = g\boldsymbol{r}$ are the transformed coordinates, i.e.,

$$f'(\boldsymbol{r}') = O(g)f(\boldsymbol{r}) = f(g^{-1}\boldsymbol{r}). \tag{15}$$

This equation tells us how to construct an operator that corresponds to a given geometrical transformation. Fig. 2 shows (15) for an atomic $x^2 - y^2$ function and a rotation by $2\pi/4$ (operation C_4); the inverse operation is the rotation by $-2\pi/4$ (operation $C_{-4} = C_4^3$).
The Hamiltonian, or any other operator $\hat{H}$, transforms as follows

$$\hat{H}' = O(g)\hat{H}O(g^{-1}). \tag{16}$$

The group of the Hamiltonian is the group of h operators $\{O(g)\}$ which leave $\hat{H}$ unchanged ($\hat{H} = \hat{H}'$), i.e., which commute with the Hamiltonian. If $\psi(\boldsymbol{r})$ is an eigenvector of the Hamiltonian with eigenvalue ε_j, then for any operator in the group of the Hamiltonian

$$O(g)\hat{H}\psi(\boldsymbol{r}) = O(g)\varepsilon_j\psi(\boldsymbol{r}) = \varepsilon_j O(g)\psi(\boldsymbol{r}) = \hat{H}O(g)\psi(\boldsymbol{r}).$$

Thus $O(g)\psi(\boldsymbol{r})$ is an eigenvector of $\hat{H}$ with eigenvalue ε_j. The wavefunctions $\{O(g)\psi(\boldsymbol{r})\}$, where the $O(g)$ are operators in the group of the Hamiltonian, are all degenerate eigenvectors of $\hat{H}$. They define a linear space $\mathcal{L}_j$ of functions $f(x) = \sum_g c_g\ O(g)\psi(\boldsymbol{r})$, where the coefficients c_g are complex numbers. The space $\mathcal{L}_j$ is invariant under the action of the operators $O(g)$ in the group of the Hamiltonian, and has dimension $d_j \leq h$. If $\mathcal{L}_j$ includes all wavefunctions with eigenvalue ε_j, the degeneracy is said to be *essential*. If there are degenerate wavefunctions which are not in $\mathcal{L}_j$, this additional degeneracy is said to be *accidental*; accidental degeneracies sometime occur because of hidden symmetries. The symmetry group of the Hamiltonian is also the symmetry group of the solid or the molecule described by the Hamiltonian. The Hamiltonian, as the physical system, is invariant under all symmetry operations in the group and therefore transforms according to the trivial irreducible representation.
Let us assume that $\{\psi_j^i(\boldsymbol{r})\}$ is a set of $d_j \leq h$ linearly independent and essentially degenerate wavefunctions with eigenvalue ε_j which span $\mathcal{L}_j$. We can then construct a d_j-dimensional

irreducible matrix representation of the group of the Hamiltonian using the set $\{\psi^i_j(\boldsymbol{r})\}$ as a basis. The matrices of this representation, $\Gamma_j(g)$, are defined formally by

$$O(g)\psi^i_j(\boldsymbol{r}) = \sum_{i'} \Gamma^{i',i}_j(g)\psi^{i'}_j(\boldsymbol{r}).$$

The function $\psi^i_j(\boldsymbol{r})$ is said to belong to the *i-th* row of the *j-th* irreducible representation. If a function $\psi^i_j(\boldsymbol{r})$ belongs to the *i-th* row of the *j-th* irreducible representation with dimensionality d_j, the remaining $d_j - 1$ functions required to complete the basis for that irreducible representations are called *partners functions* of $\psi^i_j(\boldsymbol{r})$. Two functions belonging to different irreducible representations or to different rows of the same irreducibile representations are orthogonal

$$\langle\psi^i_j|\psi^{i'}_{j'}\rangle = \delta_{i,i'}\delta_{j,j'}\frac{1}{d_j}\sum_k \langle\psi^k_j|\psi^k_j\rangle.$$

Any function $f(\boldsymbol{r})$ in the space on which a group G of operators $\{O(g)\}$ acts can be decomposed as

$$f(\boldsymbol{r}) = \sum_j^{N_j}\sum_i^{d_j} f^i_j(\boldsymbol{r}),$$

where $j = 1, \ldots, N_j$ labels all distinct irreducible representations of G, and f^i_j belongs to the *i-th* row of the *j-th* irreducible representation. The components $f^i_j(\boldsymbol{r})$ can be obtained by means of the projection operator $\hat{\mathcal{P}}^{ii}_j$

$$\hat{\mathcal{P}}^{ii}_j = \frac{d_j}{h}\sum_g \left[\Gamma^{ii}_j(g)\right]^* O(g), \tag{17}$$

$$f^i_j(\boldsymbol{r}) = \hat{\mathcal{P}}^{ii}_j f(\boldsymbol{r}).$$

The symmetry group G of the Hamiltonian can be often written as a direct product of two subgroups G_a and G_b, of dimension h_a and h_b. The *direct product* $G = G_a \otimes G_b$ is the group G with elements $\{g\}$

$$\{g\} = \{E = (e_a, e_b), g_2 = (e_a, g_{2_b}), \ldots, g_h = (g_{h_a}, g_{h_b})\},$$

with group multiplication

$$g \star g' = (g_a, g_b) \star (g'_a, g'_b) = (g_a \star g'_a, g_b \star g'_b).$$

The matrices of the irreducible representations of G, $\Gamma_j(g)$, can be constructed as direct products of the matrices of the irreducible representations of G_a and G_b, $\Gamma_{j_a}(g_a)$ and $\Gamma_{j_a}(g_b)$

$$[\Gamma_j(g)]^{i\,,i'} = [\Gamma_{j_a}(g_a)]^{i_a,i'_a} \otimes [\Gamma_{j_b}(g_b)]^{i_b,i'_b} = [\Gamma_{j_a}(g_a) \otimes \Gamma_{j_b}(g_b)]^{i_a i_b, i'_a i'_b}.$$

The character of a direct product representation is the product of the characters

$$\chi_j(g) = \chi_{j_a}(g_a)\chi_{j_b}(g_b).$$

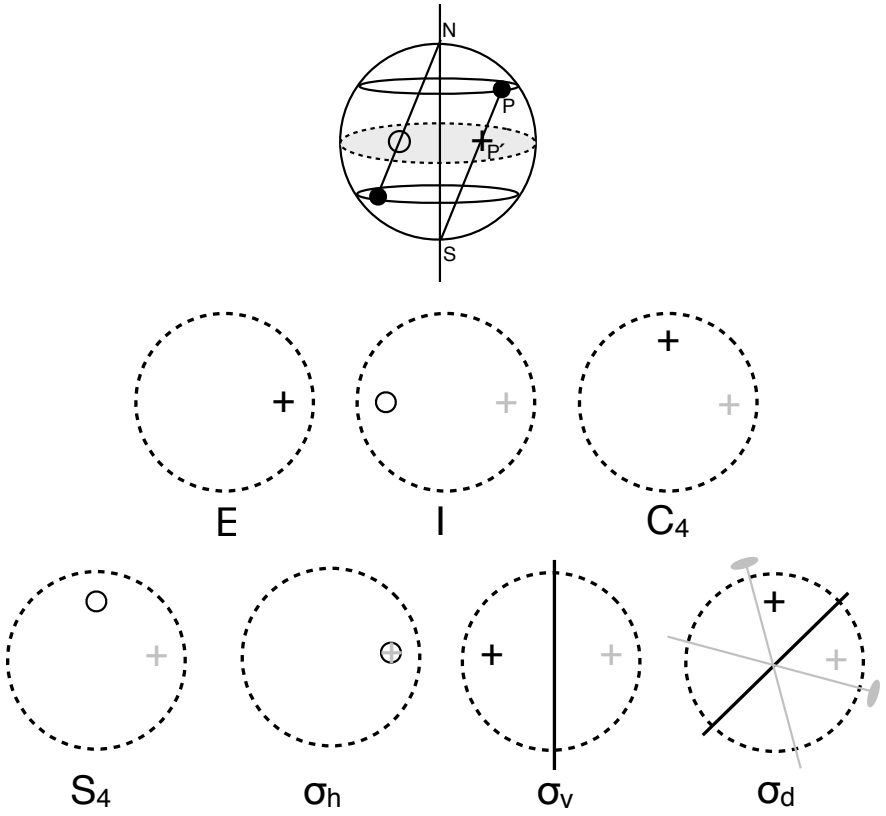

Fig. 3: *Stereographic projections illustrating the effect of some point symmetry operations. A point P at position $\mathbf{r}$ in the northern hemisphere is joint to the south pole S; the intersection of the line PS with the equatorial plane $(+)$ is P', the stereographic projection of P. To treat the two hemispheres symmetrically, a point in the southern hemisphere is projected from the north pole N; the intersection with the equatorial plane is shown as an empty circle. Let us assume that P is in the northern hemisphere. The identity operation leaves P untouched; this is shown in the picture of the equatorial circle labeled with E. The operations $g = I, C_4, S_4, \sigma_v, \sigma_h, \sigma_d$ move P (grey $+$) to position $\mathbf{r}' = g\mathbf{r}$ (black circle or black $+$); this is shown in the pictures labeled with g. For $g = \sigma_d$, the two-fold axes (labeled with a digon) are also shown. The principal axis is perpendicular to the equatorial plane.*

Let us now consider the geometrical symmetry operations and symmetry groups relevant for atoms, molecules and solids. The symmetry group of an atom (central potential) is at least $O(3) = SO(3) \otimes C_i$, where $SO(3)$ is the group of proper rotations in three dimensions and $C_i = \{E, I\}$ is the group of order two, which has the identity E and the inversion I as only elements. The group $O(3)$ includes proper rotations and improper rotations; the latter are composed operations made of rotations and inversion. For molecules and crystals, only a subset of the proper and improper rotations are covering operations. These point group operations can include

- E, the identity
- C_n, a rotation by an angle $2\pi/n$; in a crystal, n can only take the values $n = 2, 3, 4, 6$

- σ reflection in a plane, classified as
  - σ_h, reflection through a plane perpendicular to the axis of highest rotation symmetry, called *principal axis*
  - σ_v, reflection through a plane to which the principal axis belongs
  - σ_d, reflection through a plane to which the principal axis belongs, and bisecting the angle between the two-fold axes perpendicular to the principal axis.
- $S_n = \sigma_h \otimes C_n$, improper rotation of an angle $2\pi/n$; in a crystal, n can only take the values $n = 3, 4, 6$.
- $I = S_2$, the inversion.

Some of these operations are illustrated in Fig. 3 using stereographic projections.
In a crystal, additional covering operations are

- lattice translations $\boldsymbol{T} = n_1\boldsymbol{a} + n_2\boldsymbol{b} + n_3\boldsymbol{c}$, where n_i are integers and $\boldsymbol{a}$, $\boldsymbol{b}$, $\boldsymbol{c}$ the primitive translations that define the unit cell.
- glide planes and screw axes, which are made by a point group operation R and a translation of a vector $\boldsymbol{f}$ which is a fraction of a lattice vector.

The lattice translations form the *translation group*. The complete set of covering operation of a crystal is known as *space group*. In three dimensions, there are 32 crystallographic point groups and 230 space groups. An operation in the space group is indicated as $\{\boldsymbol{\tau}|R\}$, where R is an element of the point group, and $\boldsymbol{\tau}$ a translation ($\boldsymbol{\tau} = \boldsymbol{T}$ or $\boldsymbol{\tau} = \boldsymbol{f}$). Space groups which do not include glide planes or screw axes are said to be *symmorphic*; the remaining space groups are said to be *non symmorphic*.
To understand solids and molecules, it is often useful to work in a basis of atomic orbitals. Atomic functions can be used, e.g., as a starting point to construct orbitals for molecules and crystals, as in the tight-binding method. These orbitals (see Appendix B) are defined as

$$\psi_{nlm}(\rho, \theta, \phi) = R_{nl}(\rho) Y^l_m(\theta, \phi),$$

where $R_{nl}(\rho)$ is the radial function, $Y^l_m(\theta, \phi)$ a spherical harmonic, $\rho = Zr$, Z the atomic number, and nlm the quantum numbers. In a hydrogen-like atom, the states with the same principal quantum number n but different angular momentum l are degenerate. This "accidental" degeneracy is caused by a hidden symmetry[5] of the Hamiltonian of the hydrogen atom. The $(2l+1)$-fold degeneracy of a given l shell is instead essential for any system with $O(3)$ symmetry. Thus we can construct irreducible representations of $O(3)$ with dimensionality $d = 2l + 1$

[5] It can be shown that the degeneracy is associated with rotational symmetry in 4 dimensions and that the group the Hamiltonian ($1/r$ potential) is actually $O(4)$. This additional symmetry is associated with the conservation of the Laplace-Runge-Lenz (LRL) vector; a generalization of the LRL vector to the case of an arbitrary central potential also exist.

using as basis set hydrogen-like atomic functions with principal quantum number n and angular momentum quantum number l.

Let us calculate the characters of such representations. The radial function is invariant under proper and improper rotations; thus we have only to consider the effect of these operations on the spherical harmonics. According to (15), the rotation of $Y_m^l(\theta,\phi)$ about the z axis by an angle α (C_α) is equivalent to the rotation of the xy axes by $-\alpha$. Thus

$$O(C_\alpha)Y_m^l(\theta,\phi) = Y_m^l(\theta,\phi-\alpha) = e^{-im\alpha}Y_m^l(\theta,\phi).$$

Therefore the matrix $\Gamma^l(C_\alpha)$ of the d-dimensional representation Γ^l has elements

$$[\Gamma^l(C_\alpha)]_{m,m'} = \delta_{m,m'}e^{-im\alpha}.$$

The character of the representation Γ^l for a rotation C_α is then

$$\chi^l(\alpha) = \sum_{m=-l}^{l} e^{-im\alpha} = \frac{\sin(l+\frac{1}{2})\alpha}{\sin\frac{\alpha}{2}}.$$

This result is valid for any direction of the rotation axis, and for any d-dimensional basis set obtained by making linear combinations of the $Y_m^l(\theta,\phi)$ functions, because the trace of a matrix is invariant under basis transformation; in particular the result is valid for real combinations of spherical harmonics (Appendix B), the basis usually adopted to study crystals and molecules, and for a set of Wannier functions with the symmetry of spherical or a real harmonics in a given l shell. The characters of the identity and the inversion are

$$\chi^l(E) = 2l+1,$$

$$\chi^l(I) = (-1)^l(2l+1).$$

The reflection through an horizontal plane, σ_h, can be written as $\sigma_h = I \otimes C_2$; thus

$$\chi^l(\sigma_h) = (-1)^l.$$

This result is also valid for σ_v and σ_d, since it is alway possible to choose the quantization axis perpendicular to the reflection plane. Finally, an improper rotation $S_\alpha = \sigma_h \otimes C_\alpha$ can be also obtained as $S_\alpha = I \otimes C_{\alpha+\pi}$; thus

$$\chi^l(S_\alpha) = (-1)^l\frac{\sin(l+\frac{1}{2})(\alpha+\pi)}{\sin\frac{\alpha+\pi}{2}}.$$

In Tab. 1 we summarize the characters of Γ^l. Since $O(3) = SO(3)\otimes C_i$, the characters in Tab. 1 can also be obtained as product of the characters of the same representation in $SO(3)$, $\Gamma^l_{SO(3)}$, and one of the irreducible representations of the group C_i, A_g (even) and A_u (odd). The characters of $\Gamma^l_{SO(3)}$ and the table of characters of C_i are shown below

$SO(3)$	E	C_α
$\Gamma^l_{SO(3)}$	$2l+1$	$\sin(l+\frac{1}{2})\alpha/\sin\frac{\alpha}{2}$

C_i	E	I
A_g	1	1
A_u	1	-1

$O(3)$	E	C_α	I	S_α	σ
Γ^l	$2l+1$	$\sin(l+\frac{1}{2})\alpha/\sin\frac{\alpha}{2}$	$(-1)^l(2l+1)$	$(-1)^l\sin(l+\frac{1}{2})(\alpha+\pi)/\sin\frac{\alpha+\pi}{2}$	$(-1)^l$

Table 1: *Characters of the irreducible representations Γ^l of group* O(3).

The direct product representation $\Gamma^l_{SO(3)} \otimes A_g$ with l even yields Γ^l with $l = 0, 2, 4, \ldots$, while $\Gamma^l_{SO(3)} \otimes A_u$ with l odd yields Γ^l with $l = 1, 3, 5, \ldots$.
The representation Γ^l is reducible in crystallographic or molecular point groups; we can find its decomposition in irreducible representations using the decomposition formula (14). Thus Tab. 1 can be viewed as the starting point to go from atoms to molecules and crystals.

3 Crystal-field theory

In an atom, the potential $v_{\rm R}(\boldsymbol{r})$ which determines the one-electron energies (10) is central and has (at least) all the symmetries of $O(3)$. In a molecule or a solid, $v_{\rm R}(\boldsymbol{r})$ has in general lower symmetry, the symmetry of a finite point group. Thus electronic states that are degenerate in an atom can split in a solid or a molecule. The symmetry reduction arises from the *crystal field*; the latter has two components, the Coulomb potential generated by the surrounding ions and the *ligand field* due to the bonding neighbors. In this section we will analyze the first contribution; the second effect will be discussed in the next section.
Let us assume that the crystal is ionic and the ions can be treated as point charges q_α (point charge model), and let us neglect $v_{\rm H}(\boldsymbol{r})$ and $v_{\rm xc}(\boldsymbol{r})$ in (6). Then, the one-electron potential can be written as

$$v_{\rm R}(\boldsymbol{r}) = \sum_\alpha \frac{q_\alpha}{|\boldsymbol{R}_\alpha - \boldsymbol{r}|} = v_0(r) + \sum_{\alpha\neq 0} \frac{q_\alpha}{|\boldsymbol{R}_\alpha - \boldsymbol{r}|} = v_0(r) + v_c(\boldsymbol{r}), \tag{18}$$

where $\boldsymbol{R}_\alpha$ are the positions of the ions and q_α their charges. The term $v_0(r)$ is the ionic central potential at site $\boldsymbol{R}_0$, and has spherical symmetry. The term $v_c(\boldsymbol{r})$ is the electric field generated at a given site $\boldsymbol{R}_0$ by all the surrounding ions in the crystal and it is called *crystal-field potential*.
Let us consider a crystal with the perovskite structure ABC_3, shown in Fig. 4. We want to calculate the crystal-field potential at the site of the transition metal, B. Let us first assume that only the contribution of nearest neighbors (the negative C ions, usually oxygens) is relevant. The C ions are located at positions $(\pm a, 0, 0), (0, \pm a, 0), (0, 0, \pm a)$, where a is the lattice constant, and have all the same charge q_C. Expanding around $\boldsymbol{r} = 0$, we find that the first contribution to $v_{\rm c}(\boldsymbol{r})$ with less than spherical symmetry is

$$v_{\rm oct}(\boldsymbol{r}) = \frac{35}{4}\frac{q_C}{a^5}\left(x^4 + y^4 + z^4 - \frac{3}{5}r^4\right) = D\left(x^4 + y^4 + z^4 - \frac{3}{5}r^4\right).$$

We can rewrite this potential as

$$v_{\rm oct}(\boldsymbol{r}) = \frac{7}{6}\frac{1}{\sqrt{\pi}}\frac{q_C}{a^5}r^4\left[Y_0^4(\theta,\phi) + \sqrt{\frac{5}{14}}\left(Y_4^4(\theta,\phi) + Y_{-4}^4(\theta,\phi)\right)\right], \tag{19}$$

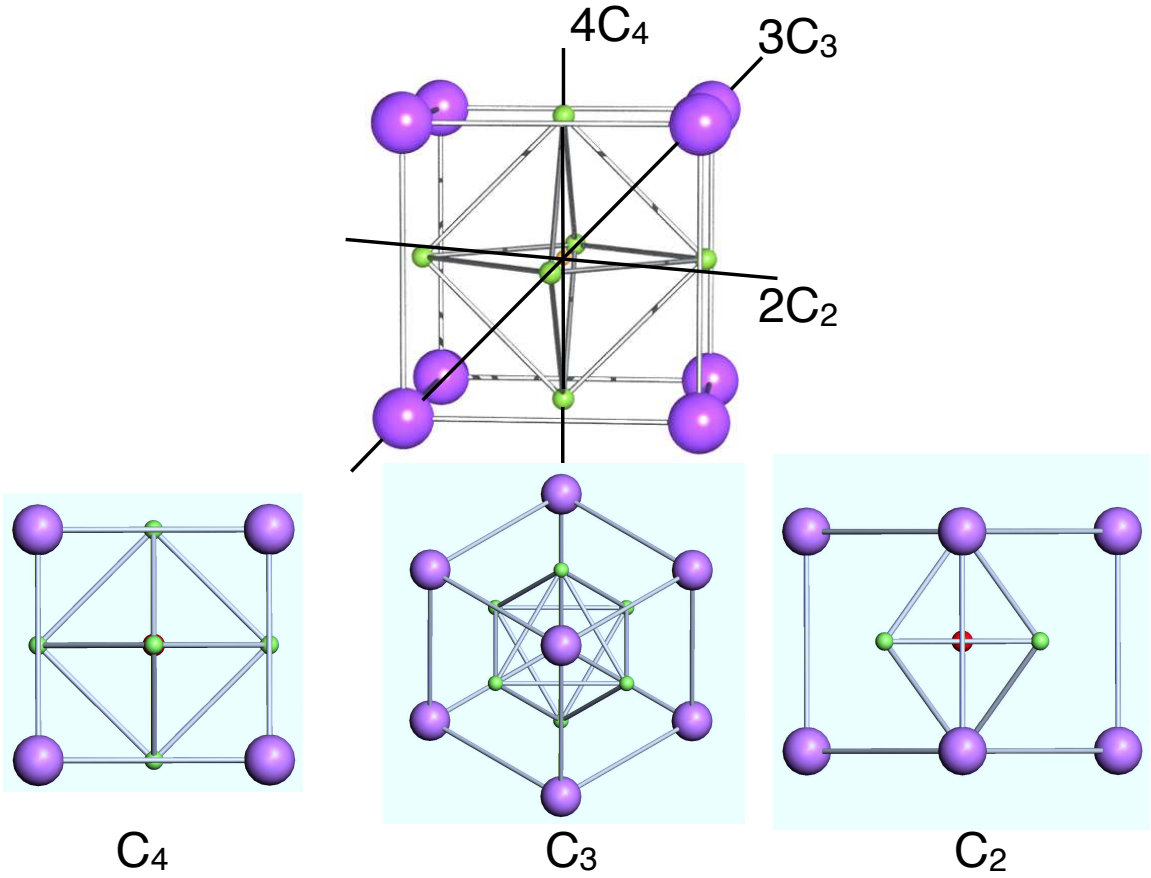

Fig. 4: *The unit cell of a cubic perovskite ABC_3 and its symmetry axes; the lattice constant is a. The transition metal B (red) is at $(0,0,0)$; the ligands C (green) are located at $(\pm a,0,0)$, $(0,\pm a,0)$,$(0,0,\pm a)$, forming an octahedron; the cations A are located at $(\pm a/2,\pm a/2,\pm a/2)$, $(\pm a/2,\mp a/2,\pm a/2)$, $(\mp a/2,\pm a/2,\pm a/2)$, $(\pm a/2,\pm a/2,\mp a/2)$, forming a cube. The bottom figures show different views illustrating the rotational symmetries of the cell.*

where

$$\begin{aligned} Y_0^4(\theta,\phi) &= \frac{3}{16}\frac{1}{\sqrt{\pi}}(35\cos^4\theta - 30\cos^2\theta + 3), \\ Y_{\pm 4}^4(\theta,\phi) &= \frac{3}{16}\frac{35}{\sqrt{2\pi}}\sin^4\theta e^{\pm 4i\phi}. \end{aligned}$$

Let us now calculate the crystal field due to the cubic cage of cations A (with charge q_A), shown in Fig. 4. One can show that

$$v_{\rm cube}(\boldsymbol{r}) = -\frac{8}{9}\frac{q_A}{q_C}v_{\rm oct}(\boldsymbol{r}),$$

i.e., $v_{\rm cube}(\boldsymbol{r})$ has the same form as $v_{\rm oct}(\boldsymbol{r})$; this happens because a cube and an octahedron are dual polyhedra[6] and have therefore the same symmetry properties. If $q_A/q_C > 0$, $v_{\rm cube}(\boldsymbol{r})$ has opposite sign than $v_{\rm oct}(\boldsymbol{r})$; however, in the case of a perovskite, cations are positive ions; thus the crystal field due to the A cage has the same sign of the field generated by the B octahedron.

[6]Every polyhedron has a dual which can be obtained by exchanging the location of faces and vertices.

The crystal-field potential $v_{\rm c}(\boldsymbol{r})$ can split the $(2l+1)$-fold degeneracy of the atomic levels. To calculate how the l manifold splits, we use group theory. We assume for simplicity that the symmetry is only O (group of the proper rotations which leave a cube invariant); using the full symmetry group of the cube, $O_h = O \otimes C_i$, does not change the result, because the spherical harmonics have fixed parity. The character table of group O is

	O	E	$8C_3$	$3C_2$	$6C_2$	$6C_4$
$(x^2+y^2+z^2)$	A_1	1	1	1	1	1
	A_2	1	1	1	-1	-1
$(x^2-y^2, 3z^2-r^2)$	E	2	-1	2	0	0
(x,y,z)	T_1	3	0	-1	-1	1
(xy,xz,yz)	T_2	3	0	-1	1	-1

(20)

We want to calculate the characters of the reducible matrix representation Γ^l constructed using spherical harmonics with quantum numbers lm as a basis. From Tab. 1

$$\begin{aligned}
\chi^l(C_2) &= (-1)^l \\
\chi^l(C_3) &= \begin{cases} 1 & l = 0,3,\ldots \\ 0 & l = 1,4,\ldots \\ -1 & l = 2,5,\ldots \end{cases} \\
\chi^l(C_4) &= \begin{cases} 1 & l = 0,1,4,5,\ldots \\ -1 & l = 2,3,6,7,\ldots \end{cases}
\end{aligned}$$

For the s,p,d,f shells we can therefore write for representations Γ^l

O	E	$8C_3$	$3C_2$	$6C_2$	$6C_4$
Γ^s	1	1	1	1	1
Γ^p	3	0	-1	-1	1
Γ^d	5	-1	1	1	-1
Γ^f	7	1	-1	-1	-1

We can now determine how the reducible representations Γ^l splits using the decomposition formula Eq. (14). Hereafter for convenience the symmetry representations of electronic terms are written in lower case to distinguish them from capital letters used for the nuclear displacements and the general irreducible representations. We find

$$\begin{aligned}
\Gamma^s &= a_1 \\
\Gamma^p &= t_1 \\
\Gamma^d &= e \oplus t_2 \\
\Gamma^f &= a_2 \oplus t_1 \oplus t_2
\end{aligned}$$

Thus, the s- and the p-functions do not split, because the a_1 irreducible representation is one-dimensional and the t_1 irreducible representation is 3-dimensional. However, d-functions split

into a doublet and a triplet, while f-functions into a singlet and two triplets. To calculate which functions belong to which representation we can, e.g., use the projector (17). For d-electrons, relevant for the case of a transition-metal ion, we find that the d-shell splits into e ($x^2-y^2, 3z^2-r^2$) and t_2 (xy, xz, yz). The partner functions for the representations of group O are given in the first column of the character table (20), on the left.

The full symmetry of the B site is O_h. The group O_h can be obtained as direct product, $O_h = O \otimes C_i$; with respect to O, the group O_h has twice the number of elements and classes, and thus twice the number of irreducible representations. The latter split into even ($a_{1g}, a_{2g}, e_g, t_{1g}, t_{2g}$) and odd ($a_{1u}, a_{2u}, e_u, t_{1u}, t_{2u}$) representations. The d-functions are even, and therefore x^2-y^2 and $3z^2-r^2$ are partners functions for the e_g irreducibile representation, while xy, xz, yz are partner functions for the t_{2g} irreducible representation. The p-orbitals are odd, and are partners functions for the t_{1u} representation.

Group theory tells us *if* the degenerate $2l+1$ levels split at a given site in a lattice, but not of *how much* they do split, and which orbitals are higher in energy. We can however calculate the crystal-field splitting approximately using (19). Let us consider first the case in which the central atom B is a transition-metal ion in a $3d^1$ configuration (e.g., Ti^{3+} or V^{4+}), which has degeneracy $2l+1=5$. In the perovskite structure, the octahedral potential $v_{\rm oct}(\boldsymbol{r})$ yields the following element of matrix between states in the d^1 manifold

$$\begin{aligned}
\langle\psi_{n20}\ |\hat{v}_{\rm oct}|\psi_{n20}\ \rangle &= +6Dq \\
\langle\psi_{n2\pm1}|\hat{v}_{\rm oct}|\psi_{n2\pm1}\rangle &= -4Dq \\
\langle\psi_{n2\pm2}|\hat{v}_{\rm oct}|\psi_{n2\pm2}\rangle &= +\ Dq \\
\langle\psi_{n2\pm2}|\hat{v}_{\rm oct}|\psi_{n2\mp2}\rangle &= +5Dq
\end{aligned}$$

where $Dq = -q_C\langle r^4\rangle/6a^5$. The crystal-field splitting between e_g and t_{2g}-states can be the obtained by diagonalizing the crystal-field matrix

$$H_{\rm CF} = \begin{pmatrix} Dq & 0 & 0 & 0 & 5Dq \\ 0 & -4Dq & 0 & 0 & 0 \\ 0 & 0 & 6Dq & 0 & 0 \\ 0 & 0 & 0 & -4Dq & 0 \\ 5Dq & 0 & 0 & 0 & Dq \end{pmatrix}.$$

We find two degenerate e_g eigenvectors with energy $6Dq$

$$\begin{aligned}
|\psi_{n20}\rangle &= |3z^2-r^2\rangle, \\
\frac{1}{\sqrt{2}}\left[|\psi_{n22}\rangle + |\psi_{n2-2}\rangle\right] &= |x^2-y^2\rangle,
\end{aligned}$$

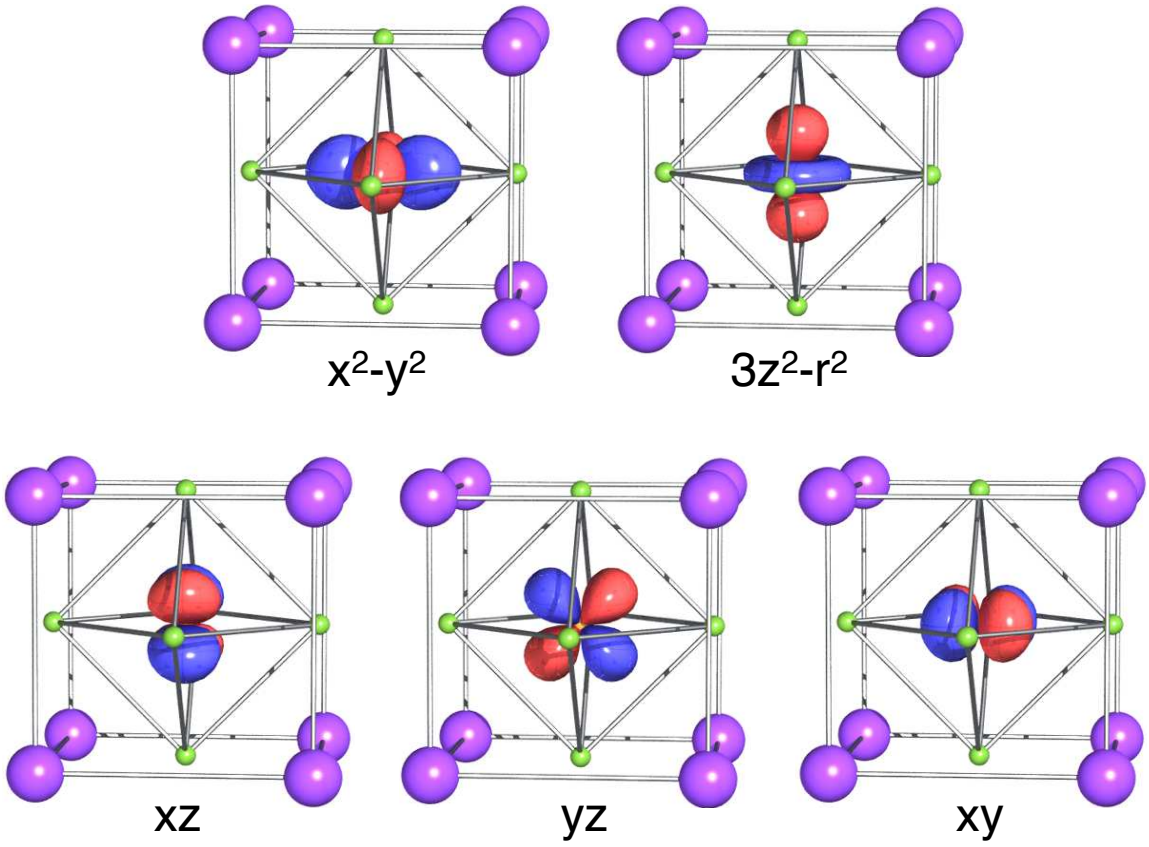

Fig. 5: *The Cu e_g and t_{2g} Wannier orbitals for the cubic perovskite $KCuF_3$, obtained from first principles calculations, using a Wannier basis that spans all bands.*

and three degenerate t_{2g} eigenvectors with energy $-4Dq$

$$\begin{aligned}
\frac{i}{\sqrt{2}}\left[|\psi_{n22}\rangle - |\psi_{n2-2}\rangle\right] &= |xy\rangle,\\
\frac{1}{\sqrt{2}}\left[|\psi_{n21}\rangle - |\psi_{n2-1}\rangle\right] &= |xz\rangle,\\
\frac{i}{\sqrt{2}}\left[|\psi_{n21}\rangle + |\psi_{n2-1}\rangle\right] &= |yz\rangle.
\end{aligned}$$

The splitting is

$$\Delta = E_{e_g} - E_{t_{2g}} = 10Dq.$$

Thus the e_g-states are higher in energy than the t_{2g}-states. This happens because e_g electrons point towards the negative C ions (see Fig. 5), and will therefore feel a larger Coulomb repulsion than t_{2g} electrons, which point between the negative C ions.
For a generic lattice, we can expand the crystal-field potential (18) in spherical harmonics using

$$\frac{1}{|\boldsymbol{r}_1 - \boldsymbol{r}_2|} = \sum_{k=0}^{\infty} \frac{r_<^k}{r_>^{k+1}} \frac{4\pi}{2k+1} \sum_{q=-k}^{k} Y_q^k(\theta_2,\phi_2)\overline{Y}_q^k(\theta_1,\phi_1),$$

where $r_<$ ($r_>$) is the smaller (larger) of r_1 and r_2. The crystal-field potential can then be written

as

$$v_c(\boldsymbol{r}) = \sum_{k=0}^{\infty} \sum_{q=-k}^{k} B_q^k Y_q^k, \tag{21}$$

where $B_q^k = (-1)^q \bar{B}_{-q}^k$. Although the series in (21) is in principle infinite, one can terminate it by specifying the wavefunctions, since

$$\langle Y_m^l | Y_q^k | Y_{m'}^l \rangle = 0 \quad \text{if} \quad k > 2l.$$

For example, for p electrons $k \leq 2$, for d-electrons, $k \leq 4$, and f electrons $k \leq 6$. Thus, for d-electrons and O_h symmetry, the terms that appear in the potential (19) are actually also the only ones to be taken into account.

The derivation of (19) and (21) presented here might let us think that the first nearest neighbors are those that determine the crystal field. However, this is often not the case, because Coulomb repulsion is a long-range interaction; for example, in some systems the first nearest neighbors yield cubic symmetry at a given site but further neighbors lower the symmetry.[7]

The point charge model discussed in this section is useful to explain the relation between crystal field and site symmetry, however yields unsatisfactory results for the crystal-field splitting in real materials. Corrections beyond the point-charge approximation turn out to be important. In addition, as we will see in the next section, in many systems the crystal field has a large, sometimes dominant, covalent contribution, the ligand field. The modern approach to calculate crystal-field splittings including the ligand-field contribution is based on material-specific DFT potentials and DFT localized Wannier functions as one-electron basis. We will discuss this approach at the end of the next section.

Let us now analyze the splitting of energy levels in a many-electron $3d^n$ manifold. Apart from the crystal field (21), in calculating the energies of states in such manifold, we have also to take into account the electron-electron Coulomb repulsion. This will be treated in detail in the lecture of Robert Eder. Here we briefly discuss some simple examples: $3d^1$, $3d^9$ and $3d^2$. We have seen that for a d-electron surrounded by an octahedron of negative ions, $\Delta = 10Dq$; the energy difference between the electronic configuration e_g^1 and electronic configuration t_{2g}^1 is therefore Δ. In the case of a single hole in the d-shell ($3d^9$ ion, e.g., Cu^{2+}), the energy difference between $t_{2g}^6 e_g^3$ and $t_{2g}^5 e_g^4$, is then just $-\Delta$, because of electron-hole symmetry. The d crystal-field orbitals (Wannier functions) for the $3d^9$ perovskite $KCuF_3$ (cubic structure) are shown in Fig. 5. For a generic $3d^n$ configuration we can consider two limit cases, strong or weak crystal field. If the crystal field is *strong*, one can treat Coulomb electron-electron interaction as a perturbation, and classify the atomic states according to the crystal field. Let us consider the case of a perovskite in which the central ion has electronic configuration $3t_{2g}^2$ (e.g., V^{3+}); if we neglect the electron-electron repulsion, the excited states are $t_{2g}^1 e_g^1$, with energy Δ, and e_g^2, with energy 2Δ. We can obtain a representation of the group O_h in the basis of two-electron states from the direct product of the representations in the basis of single-electron states. By using the decomposition

[7] This means that O_h is not the point group.

formula (14), we can then show that

$$\begin{aligned} t_{2g} \otimes t_{2g} &= a_{1g} \oplus e_g \oplus t_{1g} \oplus t_{2g} \\ e_g \otimes t_{2g} &= t_{1g} \oplus t_{2g} \\ e_g \otimes e_g &= a_{1g} \oplus a_{2g} \oplus e_g \end{aligned}$$

The Coulomb repulsion acts as a perturbation and can split degenerate states belonging to different irreducible representations. In particular, the manifold t_{2g}^2 splits into ${}^1a_{1g}$, ${}^1e_g$,${}^1\,t_{2g}$, and ${}^3t_{1g}$ (ground state), where ${}^{(2S+1)}$ indicates the spin degeneracy of the state.

If the crystal field is *weak*, the opposite approach can be used; the crystal field is treated as a perturbation of the atomic Coulomb multiplets, labeled as ${}^{2S+1}L$. In this case the two-electron ground state is the triplet ${}^3F$ and the O_h crystal field splits it into ${}^3t_{1g}$,${}^3\,t_{2g}$, and ${}^3a_{2g}$.

Up to here we have neglected the spin-orbit interaction. The latter plays an important role, e.g., in $5d$- or f-systems. In the case in which the crystal field is weak with respect to the spin-orbit coupling, as it happens in many f-electron compounds, the total angular momentum J is a good quantum number. It is therefore useful to construct a reducible representation of the point group, Γ^J, in the basis of the eigenvectors of total angular momentum. The character of Γ^J for a rotation is

$$\chi^J(\alpha) = \frac{\sin(J+\frac{1}{2})\alpha}{\sin\frac{\alpha}{2}},$$

For half-integral values of J (odd number of electrons), $\chi^J(\alpha)$ has the property

$$\chi^J(\alpha + 2\pi) = -\chi^J(\alpha).$$

We therefore expand the original point group to include a new element, R, which represents the rotation by 2π. The new group has twice the number of elements of the original group and is known as *double group*. In the case of the group O the double group is labeled with O' and its character table is

O'	E	$8C_3$	$3C_2+3RC_2$	$6C_2+6RC_2$	$6C_4$	R	$8RC_3$	$6RC_4$
Γ_1	1	1	1	1	1	1	1	1
Γ_2	1	1	1	-1	-1	1	1	-1
Γ_3	2	-1	2	0	0	2	-1	0
Γ_4	3	0	-1	-1	1	3	0	1
Γ_5	3	0	-1	1	-1	3	0	-1
Γ_6	2	1	0	0	$\sqrt{2}$	-2	-1	$-\sqrt{2}$
Γ_7	2	1	0	0	$-\sqrt{2}$	-2	-1	$\sqrt{2}$
Γ_8	4	-1	0	0	0	-4	1	0

To determine if the atomic levels in a given J manifold split we use the same procedure adopted

for the l-shell. First we calculate the characters of all elements in the group

$$\begin{aligned}
\chi^J(E) &= 2J+1 \\
\chi^J(R) &= -(2J+1) \\
\chi^J(C_2) &= 0 \\
\chi^J(RC_2) &= 0 \\
\chi^J(C_3) &= \begin{cases} 1 & J = 1/2, 7/2, \ldots \\ -1 & J = 3/2, 9/2, \ldots \\ 0 & J = 5/2, 11/2 \ldots \end{cases} \\
\chi^J(RC_3) &= \begin{cases} -1 & J = 1/2, 7/2, \ldots \\ 1 & J = 3/2, 9/2, \ldots \\ 0 & J = 5/2, 11/2 \ldots \end{cases} \\
\chi^J(C_4) &= \begin{cases} \sqrt{2} & J = 1/2, 9/2 \ldots \\ 0 & J = 3/2, 7/2, \ldots \\ -\sqrt{2} & J = 5/2, 13/2, \ldots \end{cases} \\
\chi^J(RC_4) &= \begin{cases} -\sqrt{2} & J = 1/2, 9/2 \ldots \\ 0 & J = 3/2, 7/2, \ldots \\ +\sqrt{2} & J = 5/2, 13/2, \ldots \end{cases}
\end{aligned}$$

Next we use the decomposition formula (14) to find how the reducible representation Γ^J is decomposed in irreducible ones. One can show that

$$\begin{aligned}
\Gamma^{\frac{1}{2}} &= \Gamma_6 \\
\Gamma^{\frac{3}{2}} &= \Gamma_8 \\
\Gamma^{\frac{5}{2}} &= \Gamma_7 \oplus \Gamma_8 \\
\Gamma^{\frac{7}{2}} &= \Gamma_6 \oplus \Gamma_7 \oplus \Gamma_8 \\
\Gamma^{\frac{9}{2}} &= \Gamma_6 \oplus 2\Gamma_8
\end{aligned}$$

Since $\Gamma_6, \Gamma_7, \Gamma_8$ have dimensionality $d \geq 2$, all levels remain at least two-fold degenerate. This is an example of *Kramers degeneracy*. Kramers theorem states that, in the presence of (only) electric fields, the energy levels of a system with odd number of fermions are at least two-fold degenerate. Kramers degeneracy is a consequence of time-reversal symmetry.

4 Tight-binding method

In solids, electrons delocalize to form bonds and bands. In the Hamiltonian (8), these arise from the elements of matrix (9), the hopping integrals. But what is the specific form of the Hamiltonian (8) for a given system? Which parameters are large? Which are zero? The simplest way to answer these questions is to use the tight-binding method, which consists in expanding the crystal wavefunctions in the basis of functions centered at each atomic site; here we use

as a basis atomic orbitals,[8] $\{\psi_{nlm}(\boldsymbol{r})\}$. Let us first consider a simple example, a homonuclear molecular ion formed by two hydrogen nuclei, located at $\boldsymbol{R}_1$ and $\boldsymbol{R}_2$, and one electron. The electronic Hamiltonian for such an H_2^+ molecular ion is

$$\hat{h}_e(\boldsymbol{r}) = -\frac{1}{2}\nabla^2 - \frac{1}{|\boldsymbol{r}-\boldsymbol{R}_1|} - \frac{1}{|\boldsymbol{r}-\boldsymbol{R}_2|} = -\frac{1}{2}\nabla^2 + v(\boldsymbol{r}-\boldsymbol{R}_1) + v(\boldsymbol{r}-\boldsymbol{R}_2) = -\frac{1}{2}\nabla^2 + v_R(\boldsymbol{r}).$$

We take as atomic basis the ground state $1s$ atomic orbitals, $\psi_{1s}(\boldsymbol{r}-\boldsymbol{R}_1)$ and $\psi_{1s}(\boldsymbol{r}-\boldsymbol{R}_2)$; in the free hydrogen atom they have energy ε^0_{1s}. In this basis, the Hamiltonian and the overlap matrix have the form

$$H = \varepsilon^0_{1s}\, O + \begin{pmatrix} \Delta\varepsilon_{1s} & V_{ss\sigma} \\ V_{ss\sigma} & \Delta\varepsilon_{1s} \end{pmatrix} \qquad O = \begin{pmatrix} 1 & S \\ S & 1 \end{pmatrix}$$

where

$$\begin{aligned} \Delta\varepsilon_{1s} &= \int d\boldsymbol{r}\, \psi_{1s}(\boldsymbol{r}-\boldsymbol{R}_\alpha)\left[v_R(\boldsymbol{r}) - v(\boldsymbol{r}-\boldsymbol{R}_\alpha)\right]\psi_{1s}(\boldsymbol{r}-\boldsymbol{R}_\alpha), \quad \alpha = 1,2 \\ V_{ss\sigma} &= \int d\boldsymbol{r}\, \psi_{1s}(\boldsymbol{r}-\boldsymbol{R}_\alpha) v(\boldsymbol{r}-\boldsymbol{R}_\alpha)\psi_{1s}(\boldsymbol{r}-\boldsymbol{R}_{\alpha'}), \quad \alpha \neq \alpha' \\ S &= \int d\boldsymbol{r}\, \psi_{1s}(\boldsymbol{r}-\boldsymbol{R}_\alpha)\psi_{1s}(\boldsymbol{r}-\boldsymbol{R}_{\alpha'}), \quad \alpha \neq \alpha'. \end{aligned}$$

The hopping integral $t = -V_{ss\sigma} > 0$ is a Slater-Koster two-center integral (Appendix B).
The ground state of the molecular ion is the *bonding* linear combination

$$\phi^B_{1s}(\boldsymbol{r}) = \left[\psi_{1s}(\boldsymbol{r}-\boldsymbol{R}_1) + \psi_{1s}(\boldsymbol{r}-\boldsymbol{R}_2)\right]/\sqrt{2(1+S)},$$

and has energy

$$E_B = \varepsilon^0_{1s} + \frac{\Delta\varepsilon_{1s} + V_{ss\sigma}}{1+S}.$$

The label σ in $V_{ss\sigma}$ indicates that the bonding state is symmetrical with respect to rotations about the bond axis (see Fig. 6). The excited state is the *antibonding* state

$$\phi^A_{1s}(\boldsymbol{r}) = \left[\psi_{1s}(\boldsymbol{r}-\boldsymbol{R}_1) - \psi_{1s}(\boldsymbol{r}-\boldsymbol{R}_2)\right]/\sqrt{2(1-S)},$$

and has energy

$$E_A = \varepsilon^0_{1s} + \frac{\Delta\varepsilon_{1s} - V_{ss\sigma}}{1-S}.$$

Let us now consider a crystal. If we neglect $v_{\rm H}(\boldsymbol{r})$ and $v_{\rm xc}(\boldsymbol{r})$ in (6), the one-electron Hamiltonian $\hat{h}_e(\boldsymbol{r})$ in (5) becomes

$$\hat{h}_e(\boldsymbol{r}) = -\frac{1}{2}\nabla^2 - \sum_{i,\alpha}\frac{Z_{i,\alpha}}{|\boldsymbol{r}-\boldsymbol{T}_i-\boldsymbol{R}_\alpha|} = -\frac{1}{2}\nabla^2 + \sum_{i,\alpha} v(\boldsymbol{r}-\boldsymbol{T}_i-\boldsymbol{R}_\alpha) = -\frac{1}{2}\nabla^2 + v_R(\boldsymbol{r}),$$

[8] Linear Combination of Atomic Orbitals (LCAO) approach.

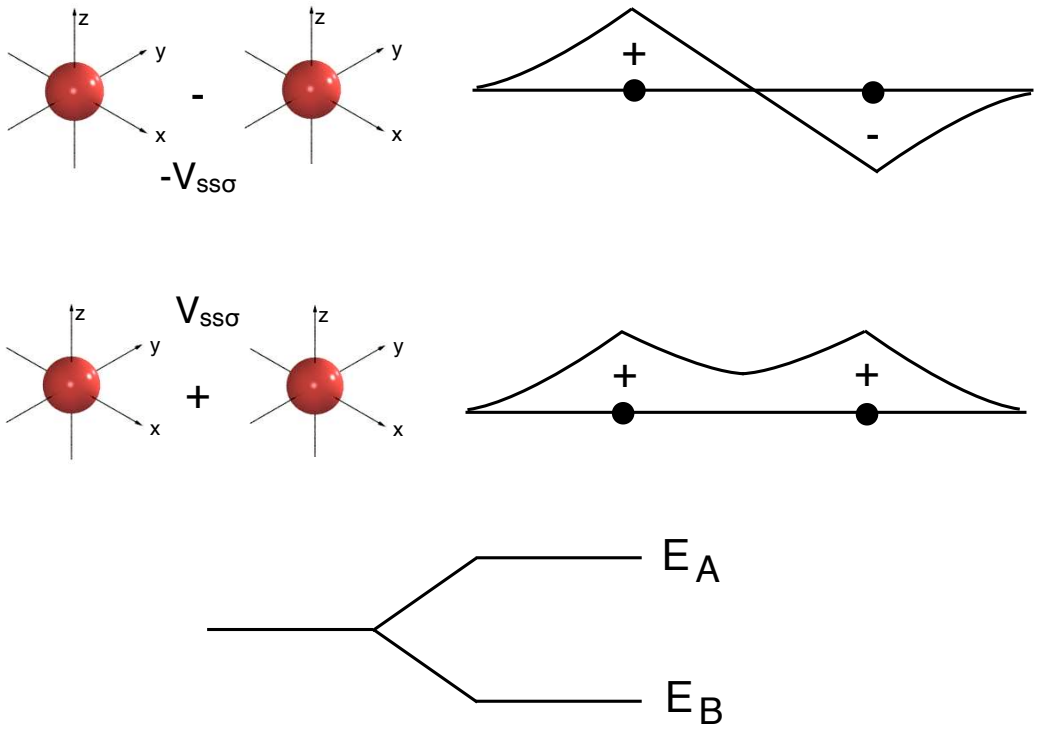

Fig. 6: *Pictorial view of the antibonding (top) and bonding (bonding) state of H_2^+.*

where $\boldsymbol{R}_\alpha$ are the positions of the basis $\{\alpha\}$ atoms in the unit cell and $\boldsymbol{T}_i$ lattice vectors. For each atomic orbital with quantum numbers lm we construct a Bloch state

$$\psi^\alpha_{lm}(\boldsymbol{k},\boldsymbol{r}) = \frac{1}{\sqrt{N}}\sum_i e^{i\boldsymbol{T}_i\cdot\boldsymbol{k}}\,\psi_{lm}(\boldsymbol{r}-\boldsymbol{T}_i-\boldsymbol{R}_\alpha). \tag{22}$$

In the Bloch basis (22), the Hamiltonian and the overlap matrix are given by

$$\begin{aligned} H^{\alpha,\alpha'}_{lm,l'm'}(\boldsymbol{k}) &= \langle\psi^\alpha_{lm}(\boldsymbol{k})|\hat{h}_e|\psi^{\alpha'}_{l'm'}(\boldsymbol{k})\rangle, \\ O^{\alpha,\alpha'}_{lm,l'm'}(\boldsymbol{k}) &= \langle\psi^\alpha_{lm}(\boldsymbol{k})|\psi^{\alpha'}_{l'm'}(\boldsymbol{k})\rangle. \end{aligned}$$

They define a generalized eigenvalue problem, the solution of which yields the band structure. The Hamiltonian matrix is given by

$$H^{\alpha,\alpha'}_{lm,l'm'}(\boldsymbol{k}) = \varepsilon^0_{l'\alpha'}O^{\alpha,\alpha'}_{lm,l'm'}(\boldsymbol{k}) + \Delta\varepsilon^\alpha_{lm,l'm'}\delta_{\alpha,\alpha'} - \frac{1}{N}\sum_{i\alpha\neq i'\alpha'} e^{i(\boldsymbol{T}_{i'}-\boldsymbol{T}_i)\cdot\boldsymbol{k}}\,t^{i\alpha,i'\alpha'}_{lm,l'm'}.$$

Here $\varepsilon^0_{l\alpha}$ are atomic levels, and $\Delta\varepsilon^\alpha_{lm,l'm'}$ the crystal-field matrix

$$\Delta\varepsilon^\alpha_{lm,l'm'} = \int d\boldsymbol{r}\,\overline{\psi}_{lm}(\boldsymbol{r}-\boldsymbol{R}_\alpha)[v_R(\boldsymbol{r}) - v(\boldsymbol{r}-\boldsymbol{R}_\alpha)]\psi_{l'm'}(\boldsymbol{r}-\boldsymbol{R}_\alpha), \tag{23}$$

which, as in the case of the H_2^+ ion, is a two-center integral. Finally

$$t^{i\alpha,i'\alpha'}_{lm,l'm'} = -\int d\boldsymbol{r}\,\overline{\psi}_{lm}(\boldsymbol{r}-\boldsymbol{R}_\alpha-\boldsymbol{T}_i)[v_R(\boldsymbol{r}) - v(\boldsymbol{r}-\boldsymbol{R}_{\alpha'}-\boldsymbol{T}_{i'})]\psi_{l'm'}(\boldsymbol{r}-\boldsymbol{R}_{\alpha'}-\boldsymbol{T}_{i'}). \tag{24}$$

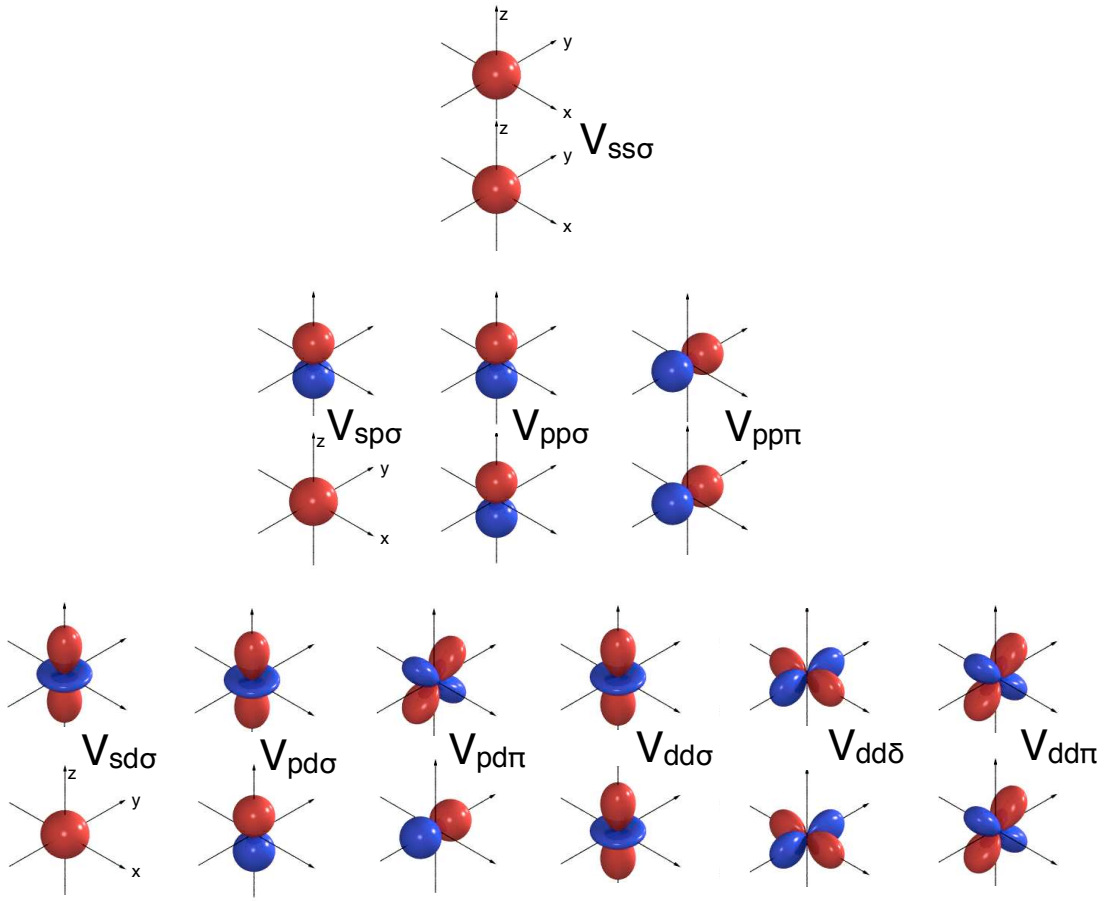

Fig. 7: *Independent Slater-Koster two-center integrals for s, p and d atomic orbitals (Appendix B). The label σ indicates that the bonding state is symmetrical with respect to rotations about the bond axis; the label π that the bond axis lies in a nodal plane; the label δ that the bond axis lies in two nodal planes.*

The hopping integrals (24) contain two-center and three-center terms; if the basis is localized, we can neglect the three-center contributions and assume that $t^{i\alpha,i'\alpha'}_{lm,l'm'} \sim -V^{i\alpha,i'\alpha'}_{lm,l'm'}$, where

$$V^{i\alpha,i'\alpha'}_{lm,l'm'} = \int d\boldsymbol{r}\, \overline{\psi}_{lm}(\boldsymbol{r}-\boldsymbol{R}_\alpha-\boldsymbol{T}_i)v(\boldsymbol{r}-\boldsymbol{R}_\alpha-\boldsymbol{T}_i)\psi_{l'm'}(\boldsymbol{r}-\boldsymbol{R}_{\alpha'}-\boldsymbol{T}_{i'})$$

is a two-center integral. A general Slater-Koster two-center integral can be expressed as a function of few independent two-center integrals, shown in Fig. 7 for s, p, and d-functions. A part from the σ bond, which is the strongest, other bonds are possible; the π bonds are made of orbitals which share a nodal plane to which the bond axis belongs, and the δ bond, which has two nodal planes which contain the bond axis and the two ions; furthermore, if the ions on the two sites are different, the bond is *polar*. Fig. 8 shows how to obtain a generic two-center integral involving p and s orbitals.

Let us now consider as an example the e_g and t_{2g} bands of $KCuF_3$; we assume for simplicity that the system is an ideal cubic perovskite (point group O_h), as in Fig. (4). Let us use as a basis only Cu d and F p atomic orbitals, and as matrix elements only on-site terms and pd hopping integrals. We label the p-orbitals on different F sites as μ^ν, where $\nu = a, b, c$ identifies

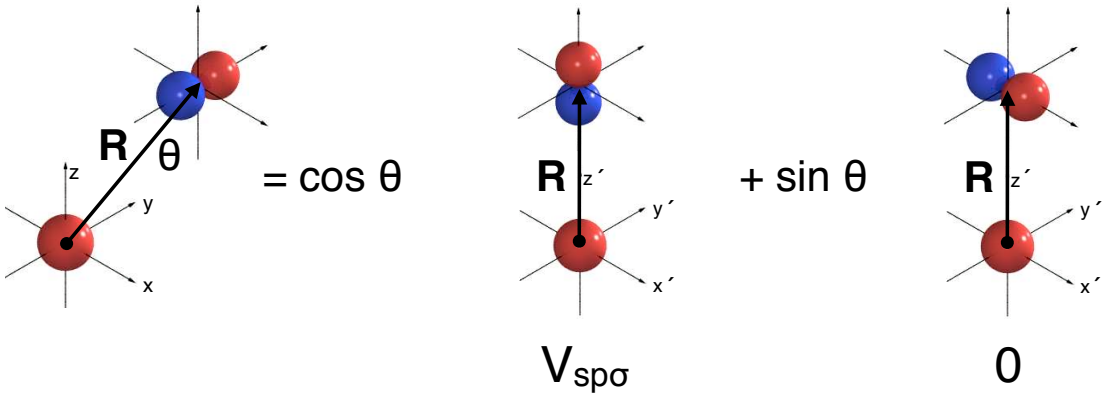

Fig. 8: *Illustration of the decomposition of a general s-p two-center integral in terms of $V_{sp\sigma}$.*

the direction of the unit cell axis along which the F atom lies and $\mu = x, y, z$ the orbital; we then construct the corresponding Bloch states $|\boldsymbol{k}\ \mu^{\nu}\rangle$, as well as the Cu e_g Bloch states $|\boldsymbol{k}\ \mu\rangle$, $\mu = 3z^2 - r^2, x^2 - y^2$. We neglect the overlap matrix for simplicity.
The tight-binding Hamiltonian in this basis has then the form

$H^{\rm TB}_{e_g}$	$\lvert\boldsymbol{k}\ z^c\rangle$	$\lvert\boldsymbol{k}\ x^a\rangle$	$\lvert\boldsymbol{k}\ y^b\rangle$	$\lvert\boldsymbol{k}\ 3z^2-r^2\rangle$	$\lvert\boldsymbol{k}\ x^2-y^2\rangle$
$\lvert\boldsymbol{k}\ z^c\rangle$	ε_p	0	0	$-2V_{pd\sigma}s_z$	0
$\lvert\boldsymbol{k}\ x^a\rangle$	0	ε_p	0	$V_{pd\sigma}s_x$	$-\sqrt{3}V_{pd\sigma}s_x$
$\lvert\boldsymbol{k}\ y^b\rangle$	0	0	ε_p	$V_{pd\sigma}s_y$	$\sqrt{3}V_{pd\sigma}s_y$
$\lvert\boldsymbol{k}\ 3z^2-r^2\rangle$	$-2V_{pd\sigma}\overline{s}_z$	$V_{pd\sigma}\overline{s}_x$	$V_{pd\sigma}\overline{s}_y$	ε_d	0
$\lvert\boldsymbol{k}\ x^2-y^2\rangle$	0	$-\sqrt{3}V_{pd\sigma}\overline{s}_x$	$\sqrt{3}V_{pd\sigma}\overline{s}_y$	0	ε_d

where $s_\alpha = ie^{-ik_\alpha a/2}\sin k_\alpha a/2$, $\alpha = x, y, z$, $\varepsilon_p < \varepsilon_d = \varepsilon_p + \Delta_{pd}$, and $V_{pd\sigma} < 0$. If $|V_{pd\sigma}|/\Delta_{pd}$ is small, the occupied bonding-like bands have mostly F p character, while the partially filled antibonding-like bands have mostly Cu e_g character. The energies ε_d and ε_p include the crystal-field term (23). We now calculate the e_g-like bands along high-symmetry lines.[9] Along the Γ-X direction we find the dispersion relations for the e_g-like bands

$$\begin{aligned} \varepsilon_2(\boldsymbol{k}) &= \varepsilon_d \\ \varepsilon_1(\boldsymbol{k}) &= \varepsilon_p + \frac{\Delta_{pd}}{2} + \frac{\sqrt{\Delta_{pd}^2 + 16V_{pd\sigma}^2|s_x|^2}}{2} \\ &\sim \varepsilon_d + 2t - 2t\cos k_x a \end{aligned} \tag{25}$$

where $t = V_{pd\sigma}^2/\Delta_{pd}$; in the last step (25) we have assumed that $|V_{pd\sigma}|/\Delta_{pd}$ is small. We can repeat the calculation for the t_{2g} bands. In this case the simplest tight-binding Hamiltonian is

$H^{\rm TB}_{t_{2g}}$	$\lvert\boldsymbol{k}\ y^a\rangle$	$\lvert\boldsymbol{k}\ x^b\rangle$	$\lvert\boldsymbol{k}\ xy\rangle$
$\lvert\boldsymbol{k}\ y^a\rangle$	ε_p	0	$2V_{pd\pi}s_x$
$\lvert\boldsymbol{k}\ x^b\rangle$	0	ε_p	$2V_{pd\pi}s_y$
$\lvert\boldsymbol{k}\ xy\rangle$	$2V_{pd\pi}\overline{s}_x$	$2V_{pd\pi}\overline{s}_y$	ε_d

[9] Special points: $\Gamma = (0,0,0)$, Z$= (0,0,\pi/a)$, X$= (\pi/a,0,0)$, M$= (\pi/a,\pi/a,0)$, R$= (\pi/a,\pi/a,\pi/a)$.

and cyclic permutations of x, y, z. In the Γ-X direction we find

$$\begin{aligned}
\varepsilon_{2'}(\boldsymbol{k}) &= \varepsilon_d \\
\varepsilon_5(\boldsymbol{k}) &= \varepsilon_p + \frac{\Delta_{pd}}{2} + \frac{\sqrt{\Delta_{pd}^2 + 16 V_{pd\pi}^2 |s_x|^2}}{2} \\
&\sim \varepsilon_d + 2t - 2t \cos k_x a
\end{aligned}$$

where $t = V_{pd\pi}^2/\Delta_{pd}$. The tight-binding model we have used so far is oversimplified, but it already qualitatively describes the e_g and t_{2g} bands in Fig. 9. A more accurate description can be obtained including other Slater-Koster integrals, such as the hopping to apical F s states, or between neighboring F p-states. With increasing number of parameters, it becomes progressively harder to estimate them, e.g. from comparison with experiments; furthermore a large number of fitting parameters makes it impossible to put a theory to a test. However, modern techniques allow us to calculate hopping integrals and crystal-field splittings *ab-initio*, using localized Wannier functions as basis instead of atomic orbitals, and the DFT potential $v_R(\boldsymbol{r})$ as one electron potential; because Wannier functions are orthogonal, the corresponding overlap matrix is diagonal. This leads to the expression (8) for the Hamiltonian, with hopping and crystal-field integrals defined as in (9) and (10).

In the simple model discussed above we could diagonalize the Hamiltonian analytically; this is, in general, not doable for models describing the full band structure of a given material in a large energy window. Group theory helps us in determining the degeneracy of states along high symmetry directions. For simplicity we first restrict ourselves to symmorphic space groups, which do not contain glide planes and screw axes; these groups are the direct product of the translational subgroup and one of the crystallographic point groups.

To understand how symmetries affect bands, we have first to introduce some new concepts. The *group of the wavevector*, $G_{\boldsymbol{k}}$, is the set of space group operations which transform $\boldsymbol{k}$ into itself or an equivalent vector $\boldsymbol{k} + \boldsymbol{G}$, where $\boldsymbol{G}$ is a reciprocal space lattice vector.

$$R\boldsymbol{k} = \boldsymbol{k} + \boldsymbol{G}.$$

The set of distinct non-equivalent vectors in $\{R\boldsymbol{k}\}$ is instead called the *star* of the $\boldsymbol{k}$ point. The group of the Γ point is the point group of the crystal, G, as every operation R transforms Γ into itself. The group of a generic $\boldsymbol{k}$ point in the first Brillouin zone is a subgroup of G, and might contain only the identity. Because the scalar product is a scalar, it is invariant under any operation. Thus

$$\boldsymbol{r} \cdot R\boldsymbol{k} = R^{-1}\boldsymbol{r} \cdot \boldsymbol{k}.$$

The effect of a point group operation on a Bloch state $\psi_{\boldsymbol{k}}(\boldsymbol{r}) = u_{\boldsymbol{k}}(\boldsymbol{r}) e^{i\boldsymbol{r}\cdot\boldsymbol{k}}$ is then

$$O(R)\psi_{\boldsymbol{k}}(\boldsymbol{r}) = O(R)u_{\boldsymbol{k}}(r)e^{i\boldsymbol{r}\cdot\boldsymbol{k}} = u_{\boldsymbol{k}}(R^{-1}\boldsymbol{r})e^{i\boldsymbol{r}\cdot R\boldsymbol{k}} = u'_{R\boldsymbol{k}}(\boldsymbol{r})e^{i\boldsymbol{r}\cdot R\boldsymbol{k}} = \psi_{R\boldsymbol{k}}(\boldsymbol{r}).$$

If $O(R)$ is in the group G of the Hamiltonian, the Bloch functions $\psi_{R\boldsymbol{k}}$ are degenerate. Under an operation in $G_{\boldsymbol{k}} \subseteq G$, the Bloch function $\psi_{\boldsymbol{k}}(\boldsymbol{r}) = u_{\boldsymbol{k}}(\boldsymbol{r}) e^{i\boldsymbol{r}\cdot\boldsymbol{k}}$ might be transformed into

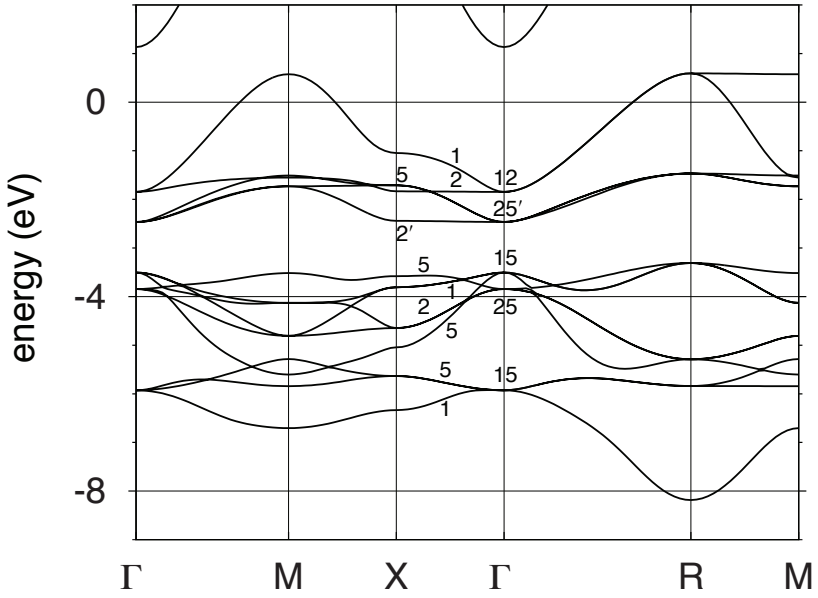

Fig. 9: *LDA band structure of cubic KCuF$_3$. Labels along the direction X-Γ indicate the corresponding irreducible representations for the e_g bands.*

a degenerate distinct function $\psi'_{\boldsymbol{k}}(\boldsymbol{r}) = u'_{\boldsymbol{k}}(\boldsymbol{r})e^{i\boldsymbol{r}\cdot\boldsymbol{k}}$ with the same wavevector; the basis of the linear space defined by the set $\{O(R)\psi_{\boldsymbol{k}}(\boldsymbol{r})\}$ builds an irreducible representation of $G_{\boldsymbol{k}}$, called the *small representation*. Thus, for symmorphic space groups, once we identified the group of the wavevector, we can use directly the character table of the point group to classify energy levels. For non-symmorphic space groups, the character table should be modified because some point group operations $\{R|0\}$ are replaced by $\{R|\boldsymbol{f}\}$; one can however show that the character for an operation $\{R|\boldsymbol{f}\}$ is $e^{i\boldsymbol{f}\cdot\boldsymbol{k}}\,\chi(R)$; at the Γ point the factor $e^{i\boldsymbol{f}\cdot\boldsymbol{k}}$ is one.
Let us analyze band-degeneracy in the case of the cubic perovskite KCuF$_3$. The space group is symmorphic and the point group is O_h; the group of the Γ point is therefore O_h. We write below the character table of O_h and the irreducible representations at the Γ point

	O_h	E	$3C_4^2$	$6C_4$	$6C_2'$	$8C_3$	I	$3IC_4^2$	$6IC_4$	$6IC_2'$	$8IC_3$
	$\Gamma_1(g)$	1	1	1	1	1	1	1	1	1	1
	$\Gamma_2(g)$	1	1	−1	−1	1	1	1	−1	−1	1
$(x^2-y^2, 3z^2-r^2)$	$\Gamma_{12}(g)$	2	2	0	0	−1	2	2	0	0	−1
(x,y,z)	$\Gamma_{15}(u)$	3	−1	1	−1	0	−3	1	−1	1	0
	$\Gamma_{25}(u)$	3	−1	−1	1	0	−3	1	1	−1	0
	$\Gamma_1'(u)$	1	1	1	1	1	−1	−1	−1	−1	−1
	$\Gamma_2'(u)$	1	1	−1	−1	1	−1	−1	1	1	−1
	$\Gamma_{12}'(u)$	2	2	0	0	−1	−2	−2	0	0	1
	$\Gamma_{15}'(g)$	3	−3	1	−1	0	3	−3	1	−1	0
(xy, xz, yz)	$\Gamma_{25}'(g)$	3	−3	−1	−1	0	3	−3	−1	−1	0

Here g are the even and u the odd representations. The e_g-bands are in the $E_g = \Gamma_{12}$ irreducible

representation, and the t_{2g} in the $T_{2g} = \Gamma'_{25}$ irreducible representation.
For a wavevector $\Delta = \frac{2\pi}{a}(k_x, 0, 0)$ the group is C_{4v}, the symmetry group of a square. The character table of point-group C_{4v} is given below

	C_{4v}	E	C_4^2	$2C_4$	$2IC_4^2$	$2IC'_2$
$1, x, 3x^2 - r^2$	Δ_1	1	1	1	1	1
$y^2 - z^2$	Δ_2	1	1	-1	1	-1
yz	Δ'_2	1	1	-1	-1	1
$yz(y^2 - z^2)$	Δ'_1	1	1	1	-1	-1
$y, z; xy, xz$	Δ_5	2	-2	0	0	0

The representations of t_{2g}-states ($T_{2g} = \Gamma'_{25}$) and that of e_g-states ($E_g = \Gamma_{12}$) in the O_h group are reducible in C_{4v} and split as follows

$$\begin{aligned} \Gamma_{12} &\to \Delta_1 \oplus \Delta_2 \\ \Gamma'_{25} &\to \Delta'_2 \oplus \Delta_5 \end{aligned}$$

Thus the e_g-states split into $3x^2 - r^2$ and $y^2 - z^2$, and the t_{2g} into yz and into xy, xz.
To analyze the F p-bands at the Γ-point, we have first to construct all 9 F p-Bloch states $|\boldsymbol{k}\ \mu^\nu\rangle$, and then construct the linear combinations which belong to specific irreducible representations of O_h. The first step is to build a reducible 9×9 odd representation, Γ^F using the states $|\boldsymbol{k}\ \mu^\nu\rangle$ as a basis. We do not need, however, to construct the full matrices, because the characters are the sum of the diagonal elements $\langle \boldsymbol{k}\ \mu^\nu | O(g) | \boldsymbol{k}\ \mu^\nu \rangle$. By adding the non-zero terms, we find

	E	$3C_4^2$	$6C_4$	$6C'_2$	$8C_3$	I	$3IC_4^2$	$6IC_4$	$6IC'_2$	$8IC_3$
Γ^F	9	-3	1	-1	0	-9	3	-1	1	0

The Γ^F representation can be decomposed in irreducible representations of the group O_h as $\Gamma^F = 2\Gamma_{15} \oplus \Gamma_{25}$. Along Γ-X the decomposition is $2\Delta_1 \oplus \Delta_2 \oplus 3\Delta_5$.
Let us now return to the crystal-field splitting. In the point charge model discussed in the previous section, the neighboring sites are viewed as ions, and their nature and tendency towards covalent bondings are ignored. In the tight-binding approach described in this section, this corresponds to calculate the terms $\Delta\varepsilon_{lm,l'm'}$ in a basis of atomic orbitals; in the simple tight-binding model considered, this gives the splitting of e_g and t_{2g} bands at the Γ point. However, the ligands do matter, because they can form bonding and antibonding states with the central atom. In the case of a cubic perovskite, the t_{2g} and e_g bands are antibonding-like bands; because $V_{pd\sigma}$ (σ bond), relevant for the e_g bands, is larger than $V_{pd\pi}$ (π bond), relevant for the t_{2g} bands, the latter are lower in energy, in agreement with the results of the point-charge model. This ligand field, differently from the crystal field in the point-charge model, is mostly determined by the first shells of neighbors, because the hopping integrals decay fast with distance (Appendix B). We can understand better the effect of the ligands by considering the e_g and t_{2g} tight-binding Hamiltonians $H^{\rm TB}_{e_g}$ and $H^{\rm TB}_{t_{2g}}$ at the $\boldsymbol{k} = M = (\pi/a, \pi/a, 0)$ point. The d-like

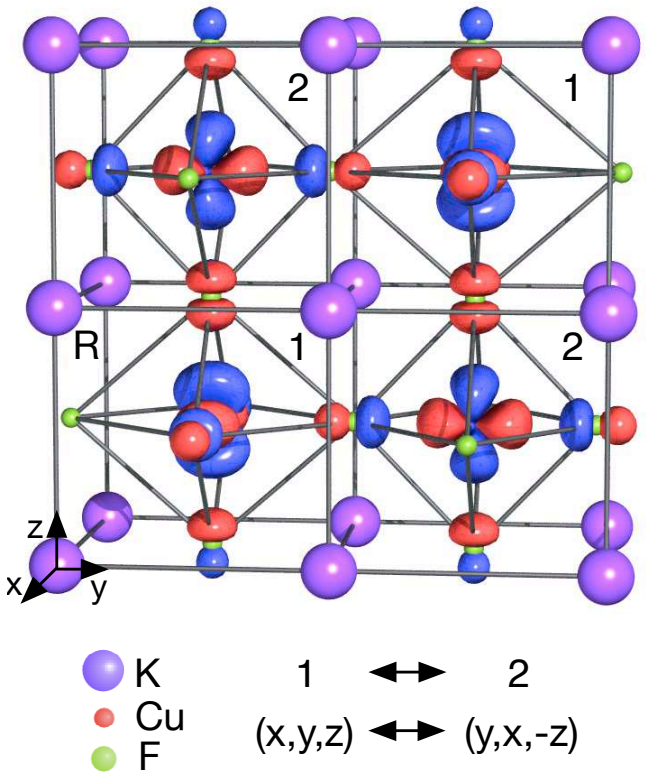

Fig. 10: *Cooperative Jahn-Teller distortion and ordering of the e_g hole orbitals in $KCuF_3$. Adapted from Ref. [7]. The Wannier function of the hole orbitals is obtained by downfolding all states but the Cu e_g; therefore, differently than the orbitals in Fig. 5, it has p-tails at F sites.*

states that diagonalize the Hamiltonians are antibonding combinations of ligand p-functions and transition-metal d-functions. Two of such states can be written as

$$\begin{aligned} |M\psi_{x^2-y^2}\rangle &= c_{1d}|M\ x^2-y^2\rangle + c_{1p}\left[|M\ x^a\rangle - |M\ y^b\rangle\right], \\ |M\psi_{xy}\rangle &= c_{2d}|M\ xy\rangle - c_{2p}\left[|M\ y^a\rangle + |M\ x^b\rangle\right], \end{aligned}$$

where c_{id}, c_{ip} define the mixing, $i = 1, 2$ and $c_{id}^2 + c_{ip}^2 = 1$. If the atomic xy and $x^2 - y^2$ orbitals are degenerate, the difference in the energy of the two states depends only on the degree of mixing and the Slater-Koster integrals $V_{pd\sigma}$ and $V_{pd\pi}$. For the simple tight-binding models presented for $KCuF_3$, the additional e_g-t_{2g} splitting due to the ligands can thus be estimated as $(W_{e_g} - W_{t_{2g}})/2$, where W_{e_g} and $W_{t_{2g}}$ are the e_g and t_{2g} band width, respectively.

As previously discussed, the modern approach to tight-binding theory consists in using localized Wannier functions, instead of atomic orbitals, as a basis. In this case, one can build Wannier functions which span the e_g and t_{2g} bands only, and which have therefore the effects of the ligands built-in. This can be seen, e.g., in Fig. 10 for the empty orbital of $KCuF_3$; the Wannier function, obtained by downfolding all states but e_g, has p tails on the neighboring F sites. In the basis of such Wannier functions, the crystal-field splitting, including ligand-field effects, can be obtained directly from the on-site elements (10) of the Hamiltonian.

5 Jahn-Teller effect

The Jahn-Teller theorem states that any electronically degenerate system can lower its energy under some structural distortions, and therefore is unstable. The only exceptions are linear molecules and Kramers degeneracy. To explain this effect we have to go back to the Born-Oppenheimer Ansatz and the system of coupled Schrödinger equations for the electrons and the lattice, (3) and (4). Let us consider a system in a high symmetry structure, $\{\boldsymbol{R}^0_\alpha\}$, for which the electronic ground state has energy $\varepsilon(\{\boldsymbol{R}^0_\alpha\})$ with degeneracy m; the corresponding degenerate electronic wavefunctions are $\psi_m(\{\boldsymbol{r}_i\};\{\boldsymbol{R}^0_\alpha\})$. Thus there are m Born-Oppenheimer potential energy surfaces $\hat{U}_n = \varepsilon(\{\boldsymbol{R}_\alpha\})$ which are degenerate for $\{\boldsymbol{R}_\alpha\} = \{\boldsymbol{R}^0_\alpha\}$. Let us consider one of these surfaces, and expand the potential around $\{\boldsymbol{R}^0_\alpha\}$. We find

$$\hat{H}_n = \hat{T}_n + \varepsilon(\{\boldsymbol{R}^0_\alpha\}) + \sum_{\alpha\mu}\left[\frac{\partial \hat{U}_n}{\partial u_{\alpha\mu}}\right]_{\{\boldsymbol{R}^0_\alpha\}} u_{\alpha\mu} + \frac{1}{2}\sum_{\alpha\mu,\alpha'\mu'}\left[\frac{\partial^2 \hat{U}_n}{\partial_{\alpha\mu}\partial_{\alpha'\mu'}}\right]_{\{\boldsymbol{R}^0_\alpha\}} u_{\alpha\mu}u_{\alpha'\mu'} + \ldots,$$

where $\boldsymbol{u}_\alpha = \boldsymbol{R}_\alpha - \boldsymbol{R}^0_\alpha$ are displacement vectors, and $\mu = x, y, z$. If $\{\boldsymbol{R}^0_\alpha\}$ is an equilibrium structure, the gradient is zero. In this case, the Hamiltonian can be written as

$$\hat{H}_n \sim \hat{T}_n + \frac{1}{2}\sum_{\alpha\mu,\alpha'\mu'}\left[\frac{\partial^2 \hat{U}_n}{\partial_{\alpha\mu}\partial_{\alpha'\mu'}}\right]_{\{\boldsymbol{R}^0_\alpha\}} u_{\alpha\mu}u_{\alpha'\mu'} + \cdots = \hat{T}_n + \hat{U}^{\rm PH}_n(\{\boldsymbol{R}^0_\alpha\}) + \ldots, \tag{26}$$

where we have defined $\varepsilon(\{\boldsymbol{R}^0_\alpha\})$ as the energy zero. It is convenient to rewrite (26) in *normal coordinates* $\{Q_{\beta\nu}\}$ and associated canonically conjugated momenta $\{P_{\beta\nu}\}$. The normal coordinates are the linear combination of displacements, $Q_{\beta\nu} = \sum_{\alpha\mu} a_{\beta\nu,\alpha\mu}u_{\alpha\mu}$, with $\beta = 1,\ldots N_n$, $\nu = x, y, z$, which bring (26) in the diagonal form

$$\hat{H}_n \sim \frac{1}{2}\sum_{\beta\nu}(P^2_{\beta\nu} + \omega^2_{\beta\nu}Q^2_{\beta\nu}). \tag{27}$$

In a crystal, this Hamiltonian yields the phonon dispersions. In general, the high-symmetry structure might or might not be a stationary point. The behavior of the energy surfaces close to the high symmetry point in which they are degenerate allows us to separate them into two classes, the first one in which $\{\boldsymbol{R}^0_\alpha\}$ is a stationary point for all m (Renner-Teller intersection), and the second in which the surface is not a stationary point at least for some of the surfaces (Jahn-Teller intersection). The classical Jahn-Teller systems are those for which $\nabla\hat{U}_n(\{\boldsymbol{R}^0_\alpha\}) \neq 0$ at least in some direction (see, e.g., Fig. (11)). Let us now consider the first order correction to the m degenerate eigenvalues due to a small distortion around $\{\boldsymbol{R}^0_\alpha\}$. The electronic Hamiltonian (3) has matrix elements

$$\begin{aligned}\langle\psi_m|\hat{H}_e(\{\boldsymbol{R}_\alpha\})|\psi_{m'}\rangle &= \varepsilon(\{\boldsymbol{R}^0_\alpha\}) + \sum_{\alpha\mu}\langle\psi_m|\left[\frac{\partial \hat{H}_e}{\partial u_{\alpha\mu}}\right]_{\{\boldsymbol{R}^0_\alpha\}}|\psi_{m'}\rangle u_{\alpha\mu} + \ldots \\ &= \varepsilon(\{\boldsymbol{R}^0_\alpha\}) + \hat{U}^{\rm JT}_{m,m'} + \ldots.\end{aligned}$$

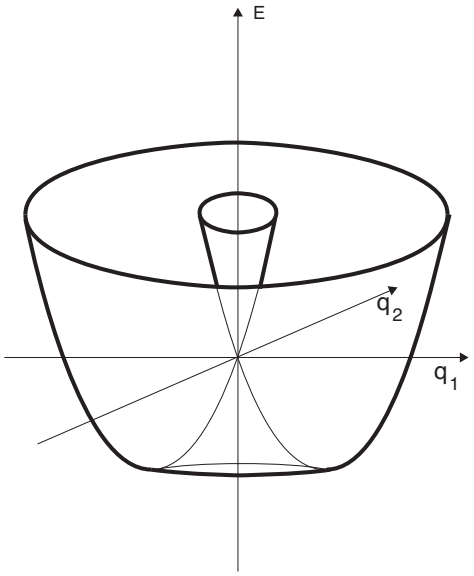

Fig. 11: *Born-Oppenheimer potential-energy surface exhibiting the form of a mexican hat. The slope of the curve at small distortions q_1, q_2 yields the Jahn-Teller coupling constant λ.*

Since the perturbation $\hat{U}^{\rm JT}$ couples the degenerate functions, we generalize the Born-Oppenheimer Ansatz as follows

$$\Psi(\{\boldsymbol{r}_i\},\{\boldsymbol{R}_\alpha\}) \;=\; \sum_m \psi_m(\{\boldsymbol{r}_i\};\{\boldsymbol{R}_\alpha\})\Phi_m(\{\boldsymbol{R}_\alpha\}).$$

To find the equations for the functions $\{\hat{\Phi}_m\}$, we write the Schödinger equation $H\Psi = E\Psi$, multiply on the left by $\overline{\psi}_m$, and integrate over the coordinates of the electrons.[10] We obtain

$$\hat{H}_n\Phi_m(\{\boldsymbol{R}_\alpha\}) = [\hat{T}_n + \hat{U}_n^{\rm PH}]\Phi_m(\{\boldsymbol{R}_\alpha\}) + \sum_{m,m'} U^{\rm JT}_{m,m'}\Phi_{m'}(\{\boldsymbol{R}_\alpha\}) = E\Phi_m(\{\boldsymbol{R}_\alpha\}). \qquad (28)$$

The Jahn-Teller potential couples degenerate Born-Oppenheimer sheets, and the dynamic of the system close to the degeneracy point is determined by all degenerate sheets. The ground state of (28) yields a new structure $\{\tilde{\boldsymbol{R}}^0_\alpha\}$ in which the electronic states are not any more degenerate. Let us consider a classical example of a Jahn-Teller material, $KCuF_3$. In the high-symmetry cubic perovskite structure shown in Fig. 12, the two Cu $3d^9$ configurations with a hole in one of the e_g orbitals ($3t_{2g}^6e_g^3$ states), are degenerate. The Jahn-Teller theorem tells us that there must be a geometrical instability. Let us consider a single octahedron and the normal modes that could lead to such an instability through coupling to the e_g-states. These are the modes Q_1 and Q_2 shown in Fig. 12. They are defined as

$$\begin{aligned}\boldsymbol{Q}_1 &= [\boldsymbol{u}_1(q_1) - \boldsymbol{u}_4(q_1) - \boldsymbol{u}_2(q_1) + \boldsymbol{u}_5(q_1)],\\ \boldsymbol{Q}_2 &= [\boldsymbol{u}_3(q_2) - \boldsymbol{u}_6(q_2) - \boldsymbol{u}_1(q_2) + \boldsymbol{u}_4(q_2) - \boldsymbol{u}_2(q_2) + \boldsymbol{u}_5(q_2)],\end{aligned}$$

[10] We neglect non adiabatic corrections, i.e., the operator $\hat{\Lambda}_n$, with elements $\langle m|\hat{\Lambda}_n|m'\rangle = -\sum_\alpha \frac{1}{M_\alpha}\left[\frac{1}{2}\langle\psi_m|\nabla^2_\alpha\psi_{m'}\rangle + \langle\psi_m|\nabla_\alpha\psi_{m'}\rangle\cdot\nabla_\alpha\right]$

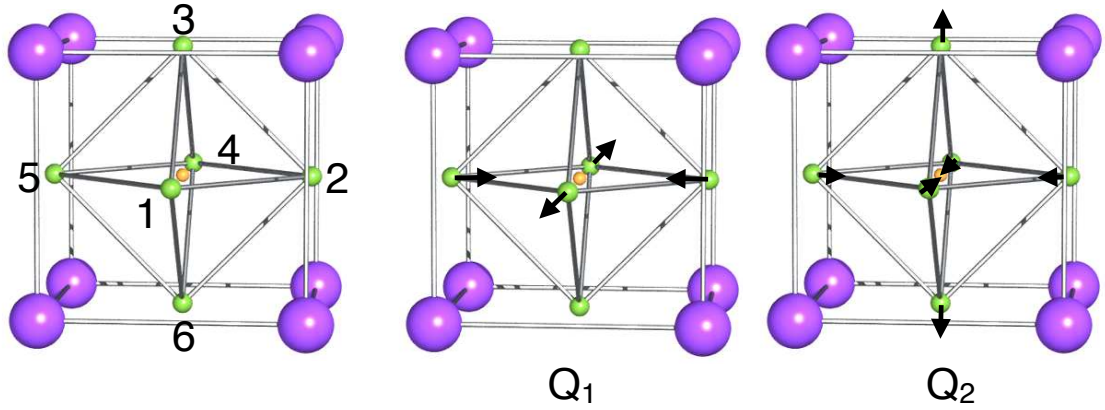

Fig. 12: *Unit cell (left) and degenerate vibrational modes Q_1 and Q_2 of cubic $KCuF_3$.*

where the displacements are

$$\begin{array}{rclrcl}
\boldsymbol{u}_1(q_1) &=& \frac{1}{\sqrt{2}}q_1(1,0,0) & \boldsymbol{u}_1(q_2) &=& -\frac{1}{\sqrt{6}}q_2(1,0,0)\\
\boldsymbol{u}_2(q_1) &=& -\frac{1}{\sqrt{2}}q_1(0,1,0) & \boldsymbol{u}_2(q_2) &=& -\frac{1}{\sqrt{6}}q_2(0,1,0)\\
\boldsymbol{u}_3(q_1) &=& (0,0,0) & \boldsymbol{u}_3(q_2) &=& \frac{2}{\sqrt{6}}q_2(0,0,1)\\
\boldsymbol{u}_4(q_1) &=& -\frac{1}{\sqrt{2}}q_1(1,0,0) & \boldsymbol{u}_4(q_2) &=& \frac{1}{\sqrt{6}}q_2(1,0,0)\\
\boldsymbol{u}_5(q_1) &=& \frac{1}{\sqrt{2}}q_1(0,1,0) & \boldsymbol{u}_5(q_2) &=& \frac{1}{\sqrt{6}}q_2(0,1,0)\\
\boldsymbol{u}_6(q_1) &=& (0,0,0) & \boldsymbol{u}_6(q_2) &=& -\frac{2}{\sqrt{6}}q_2(0,0,1)
\end{array}$$

For the Q_1 and Q_2 modes, the quadratic potential has the form

$$\hat{U}_n^{\rm PH} = \frac{1}{2}C(q_1^2+q_2^2).$$

$KCuF_3$ is thus an example of a $e\otimes E$ Jahn-Teller system, a system in which an electronic doublet (e) interacts with a doublet of degenerate normal modes (E). The form[11] of the Jahn-Teller potential $\hat{U}^{\rm JT}$ can be obtained from the effect of the perturbation due to Q_1 and Q_2 on the crystal-field matrix (23). The linear order correction is

$$\Delta\varepsilon_{lm,l'm'}(\mathbf{0},\boldsymbol{R}_\alpha+\boldsymbol{u}) - \Delta\varepsilon_{lm,l'm'}(\mathbf{0},\boldsymbol{R}_\alpha) \sim \nabla\Delta\varepsilon_{lm,l'm'}(\mathbf{0},\boldsymbol{R}_\alpha)\cdot\boldsymbol{u}$$

For e_g-states we use for simplicity the following approximations[12]

$$\begin{aligned}
\Delta\varepsilon_{3z^2-r^2,3z^2-r^2} &\sim \left[n^2-\frac{1}{2}(l^2+m^2)\right]^2\tilde{V}_{dd\sigma},\\
\Delta\varepsilon_{3z^2-r^2,x^2-y^2} &\sim \frac{\sqrt{3}}{2}(l^2-m^2)\left[n^2-\frac{1}{2}(l^2+m^2)\right]\tilde{V}_{dd\sigma},\\
\Delta\varepsilon_{x^2-y^2,x^2-y^2} &\sim \frac{3}{4}(l^2-m^2)^2\tilde{V}_{dd\sigma}.
\end{aligned}$$

[11] The covalent contribution yields the same form of the potential.

[12] The crystal-field integrals are also two-center integrals; the table of Slater-Koster integrals in Appendix B is thus still valid, provided that $V_{ll'\alpha}$ are replaced by the corresponding crystal-field terms, which we indicate as $\tilde{V}_{ll'\alpha}$.

By summing all relevant contributions, we obtain

$$\hat{U}^{\rm JT}(q_1,q_2) = -\lambda \begin{pmatrix} q_2 & q_1 \\ q_1 & -q_2 \end{pmatrix} = -\lambda\left(q_1\hat{\tau}_x + q_2\hat{\tau}_z\right), \quad \lambda \propto |\tilde{V}'_{dd\sigma}|$$

where λ is the Jahn-Teller coupling and $\hat{\tau}_z$, $\hat{\tau}_x$ are pseudospin operators in orbital space, with

$$\begin{array}{llll} \hat{\tau}_z|3z^2-r^2\rangle & = -|3z^2-r^2\rangle, & \hat{\tau}_z|x^2-y^2\rangle & = |x^2-y^2\rangle, \\ \hat{\tau}_x|3z^2-r^2\rangle & = \ \ |x^2-y^2\rangle, & \hat{\tau}_x|x^2-y^2\rangle & = |3z^2-r^2\rangle. \end{array}$$

In matrix form

$$\hat{\tau}_z = \begin{pmatrix} 1 & 0 \\ 0 & -1 \end{pmatrix} \quad \hat{\tau}_x = \begin{pmatrix} 0 & 1 \\ 1 & 0 \end{pmatrix}.$$

If we neglect the kinetic energy of the nuclei (limit $M_\alpha \to \infty$), the ground state of the system can be obtained minimizing the potential energy

$$U(q_1,q_2) = \hat{U}^{\rm JT} + \hat{U}_n^{\rm PH} = -\lambda \begin{pmatrix} q_2 & q_1 \\ q_1 & -q_2 \end{pmatrix} + \frac{1}{2}C(q_1^2+q_2^2). \tag{29}$$

To find the minimum of (29), it is convenient to introduce polar coordinates, which we define as $q_2 = q\cos\theta, q_1 = q\sin\theta$. In these coordinates

$$U^{\rm JT} = -\lambda q \begin{pmatrix} \cos\theta & \sin\theta \\ \sin\theta & -\cos\theta \end{pmatrix}.$$

We find two eigenvalues; the lowest energy branch $E(q) = -\lambda q + \frac{1}{2}q^2$ takes the form of a mexican hat, shown in Fig. 11. The minimum of $E(q)$ is obtained for $q = q_0 = \lambda/C$ and has value $E_{\rm JT} = -\lambda^2/2C$; the quantity $E_{\rm JT}$ is defined as the Jahn-Teller energy of the system. The electronic ground state can be written as

$$|\theta\rangle_G = -\sin\frac{\theta-\pi}{2}|x^2-y^2\rangle + \cos\frac{\theta-\pi}{2}|3z^2-r^2\rangle.$$

The excited state (hole orbital), with energy $\lambda q + \frac{1}{2}q^2$, is

$$|\theta\rangle_E = -\sin\frac{\theta}{2}|x^2-y^2\rangle + \cos\frac{\theta}{2}|3z^2-r^2\rangle.$$

The states $|\theta\rangle_E$ with different θ are shown in Fig. 13. In the simple model discussed so far, all states $|\theta\rangle_G$ have the same Jahn-Teller energy. Cubic symmetry however only requires that θ, $\theta + 2\pi/3$, and $\theta - 2\pi/3$ yield degenerate states. The additional degeneracy is removed when we take into account anharmonic terms, the lowest order of which has the form

$$U^{\rm anh}(q_1,q_2) = -\beta(Q_2^3 - 3Q_2Q_1^2) \propto \cos 3\theta,$$

and yields, for positive β, the tetragonal distortions ($\theta = 0, \pm 2\pi/3$) as ground state configuration. Higher order terms or a negative β can reverse the sign of the potential, making the Q_1 Jahn-Teller distortion ($\theta = 2\pi/4, 2\pi/4 \pm 2\pi/3$) more stable [8].

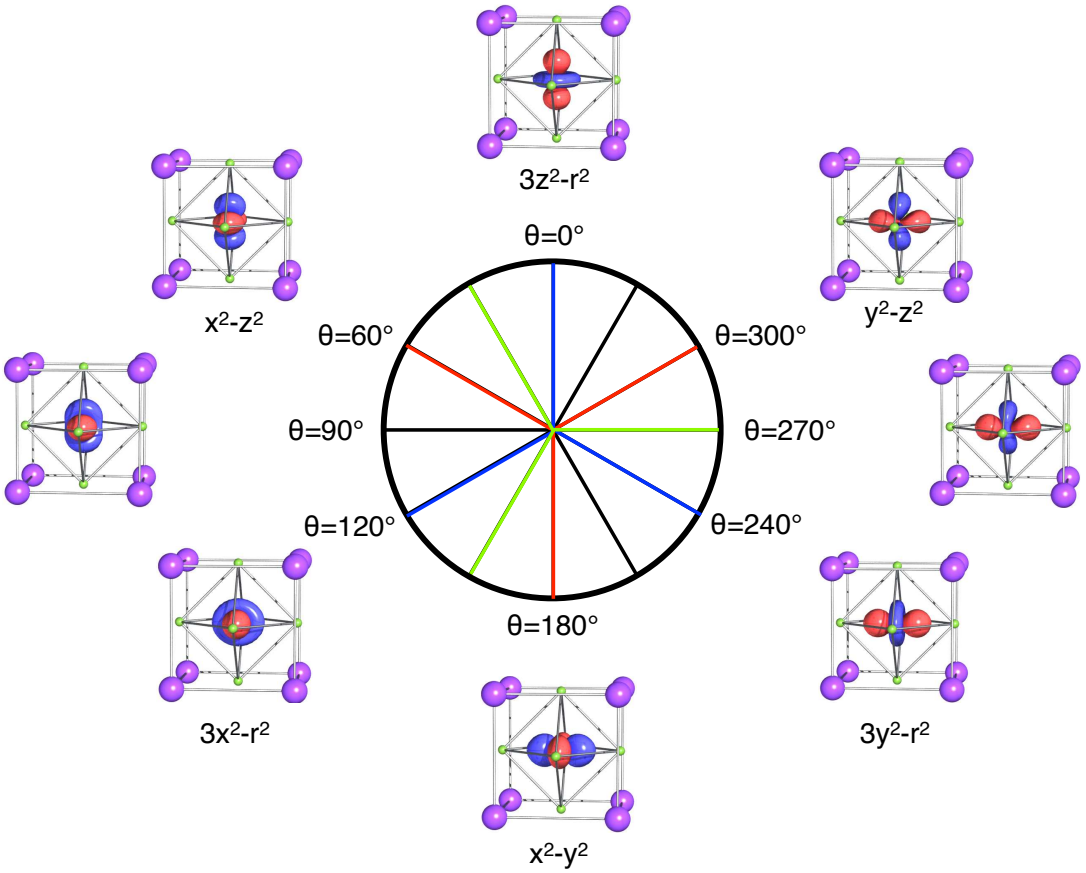

Fig. 13: *Linear combinations of e_g-states, $|\theta\rangle = -\sin\frac{\theta}{2}|x^2-y^2\rangle + \cos\frac{\theta}{2}|3z^2-r^2\rangle$. The $\theta = 0^o$ orbital is the excited state in the presence of a tetragonal compression along the z axis, while $\theta = \pm 2\pi/3$ are excited states for a tetragonal compression along x or y. This three-fold degeneracy (rotation of $\pm 2\pi/3$) is due to cubic symmetry.*

In the presence of Jahn-Teller distortions and/or many-body super-exchange effects, orbital-order phenomena can take place. Super-exchange phenomena are discussed in the lecture of Erik Koch. The order of orbitals in $KCuF_3$, calculated using the LDA+DMFT approach, is shown in Fig. 10. The origin of orbital order in $KCuF_3$ and $LaMnO_3$, and the related interplay between Jahn-Teller effect and many-body super-exchange, are discussed in Refs. [7, 9].

Let us now analyze the different electronic configurations that can occur in perovskites. For the electronic configuration $3d^1 = 3t_{2g}^1$, the procedure is as the one illustrated above, except that t_{2g}-states are 3-fold degenerate and form π bonds, which are weaker, therefore the splitting introduced by the Jahn-Teller effect is smaller than for e_g-states. In the case of electronic configurations $3d^n$ with $n > 1$, to determine if the ion is Jahn-Teller active one has to consider the degeneracies of the many-body state, including Coulomb repulsion. Weak Jahn-Teller states are $3d^1$ (Ti^{3+} in $LaTiO_3$) and $3d^2$ (V^{3+} in $LaVO_3$), as also $3t_{2g}^4$, $3t_{2g}^5$, $3t_{2g}^4 e_g^2$, $3t_{2g}^5 e_g^2$; strong Jahn-Teller configurations are, e.g., $3d^9$ (Cu^{2+} in $KCuF_3$) and $3t_{2g}^3 e_g^1$ (Mn^{3+} in $LaMnO_3$); the configurations $3t_{2g}^3$ and $3t_{2g}^3 e_g^2$ are not degenerate and therefore not Jahn-Teller active.

6 Conclusions

The parameters of the one-electron Hamiltonian are essential ingredients of many-body models. The crystal-field splittings and the hopping integrals carry the information on the lattice and the covalency, and determine to a large extent what makes a system different from the others. The color of a transition-metal complex is for example often determined by the e_g-t_{2g} crystal-field splitting. For a given system, the hopping integrals determine the band structure and the shape of the Fermi surface; the crystal-field splitting plays a crucial role for the local properties, such as the local magnetic moments or spin states, competing with spin-orbit interaction and Coulomb repulsion. In strongly correlated systems, the competition between hopping integrals and Coulomb interaction decides if the system is a metal or a Mott insulator; the crystal-field splitting can however help the formation of a Mott insulating state by reducing the degeneracy of the relevant many-body states [2].

In this lecture we have discussed simple approaches to determine the one-electron parameters for a given system. Such approaches are based on atomic orbitals and symmetries. They are easier to use for high-symmetry systems, in which the number of parameters to determine are small; once the model is constructed, the parameters can be obtained, e.g., by fitting to experiment. In the age of massively parallel supercomputers and standard *ab-initio* codes, it might seem anachronistic to study approximate methods to calculate one-electron parameters. However, these approaches are very useful for understanding qualitatively the behavior of a given system, and the results of complex calculations. It is indeed astonishing how far we can often go in understanding a system with these methods alone. One of the reasons of the successes of tight-binding and crystal-field theory is that symmetries are fully accounted for. In developing approximations to describe numerically complex many-body effects, we should always remember that symmetries are crucial, and taking them into account is essential to understand the properties of a given material.

The modern approach to calculate one-electron parameters is based on *ab-initio* localized Wannier functions; they are built from DFT calculations (e.g., in the LDA approximation), and used as a one-electron basis to construct material-specific many-body models. The choice of LDA Wannier functions as a basis relies on the success of the LDA in describing the properties of weakly correlated systems. These successes let us hope that the long-range and the mean-field part of the electron-electron interaction are already well accounted for by the LDA. Thanks to *ab-initio* Wannier functions it is possible to build many-body models even for low-symmetry materials, accounting, e.g., for the effects of small distortions that split the t_{2g} levels [2], a very hard task with semiempirical tight binding. When using Wannier functions as a one-electron basis to build many-body models, we should however never forget what are the assumptions behind; simple models and symmetry considerations remind us where all comes from.

Acknowledgment

Support of the Deutsche Forschungsgemeinschaft through FOR1346 is gratefully acknowledged.

Appendices

A Constants and units

In this lecture, formulas are given in atomic units. The unit of mass m_0 is the electron mass ($m_0 = m_e$), the unit of charge e_0 is the electron charge ($e_0 = e$), the unit of length a_0 is the Bohr radius ($a_0 = a_B \sim 0.52918$ Å), and the unit of time is $t_0 = 4\pi\varepsilon_0\hbar a_0/e^2$. In these units, m_e, a_B, e and $1/4\pi\varepsilon_0$ have the numerical value 1, the speed of light is $c = 1/\alpha \sim 137$, and the unit of energy is $1\text{Ha} = e^2/4\pi\varepsilon_0 a_0 \sim 27.211$ eV.

B Atomic orbitals

B.1 Radial functions

The nlm hydrogen-like atomic orbital is given by

$$\psi_{nlm}(\rho,\theta,\phi) = R_{nl}(\rho)Y_l^m(\theta,\phi),$$

where $R_{nl}(\rho)$ is the radial function and $Y_m^l(\theta,\phi)$ a spherical harmonic, $\rho = Zr$ and Z the atomic number. In atomic units, the radial functions are

$$R_{nl}(\rho) = \sqrt{\left(\frac{2Z}{n}\right)^3 \frac{(n-l-1)!}{2n[(n+l)!]^3}} e^{-\rho/n} \left(\frac{2\rho}{n}\right)^l L_{n-l-1}^{2l+1}\left(\frac{2\rho}{n}\right),$$

where L_{n-l-1}^{2l+1} are generalized Laguerre polynomials of degree $n-l-1$.
The radial function for $n = 1, 2, 3$ are

$$\begin{aligned}
R_{1s}(\rho) &= 2 \; Z^{3/2} && e^{-\rho} \\
R_{2s}(\rho) &= \tfrac{1}{2\sqrt{2}} \; Z^{3/2} && (2-\rho)\, e^{-\rho/2} \\
R_{2p}(\rho) &= \tfrac{1}{2\sqrt{6}} \; Z^{3/2} && \rho\, e^{-\rho/2} \\
R_{3s}(\rho) &= \tfrac{2}{3\sqrt{3}} \; Z^{3/2} && (1-2\rho/3+2\rho^2/27)\, e^{-\rho/3} \\
R_{3p}(\rho) &= \tfrac{4\sqrt{2}}{9\sqrt{3}} \; Z^{3/2} && \rho(1-\rho/6)\, e^{-\rho/3} \\
R_{3d}(\rho) &= \tfrac{2\sqrt{2}}{81\sqrt{15}} \; Z^{3/2} && \rho^2\, e^{-\rho/3}
\end{aligned}$$

where we used the standard notation s for $l = 0$, p for $l = 1$ and d for $l = 2$.

B.2 Real harmonics

To study solids, it is usually convenient to work in the basis of real harmonics. The latter are defined in terms of the spherical harmonics as follows:

$$y_{l0} = Y_0^l, \quad y_{lm} = \frac{1}{\sqrt{2}}(Y_{-m}^l + (-1)^m Y_m^l), \quad y_{l-m} = \frac{i}{\sqrt{2}}(Y_{-m}^l - (-1)^m Y_m^l), \quad m > 0.$$

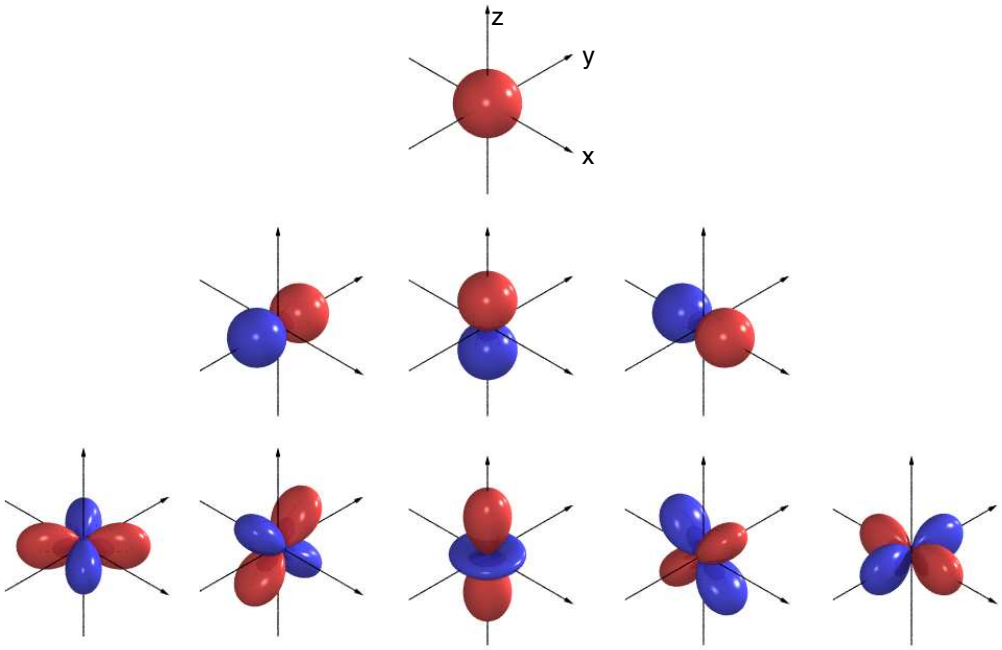

Fig. 14: *The s (first row), p_y, p_z, p_x (second row), and d_{xy}, d_{yz}, $d_{3z^2-r^2}$, d_{xz}, $d_{x^2-y^2}$ (last row) real harmonics.*

Using the definitions $x = r\sin\theta\cos\phi$, $y = r\sin\theta\sin\phi$, $z = r\cos\theta$, we can express the $l = 0, 1, 2$ real harmonics (Fig. 14) as

$$
\begin{aligned}
s \quad &= y_{00} \quad = Y_0^0 \qquad\qquad = \sqrt{\tfrac{1}{4\pi}} \\
p_y \quad &= y_{1-1} = \tfrac{i}{\sqrt{2}}(Y_1^1 + Y_{-1}^1) = \sqrt{\tfrac{3}{4\pi}} \qquad y/r \\
p_z \quad &= y_{10} \quad = Y_2^0 \qquad\qquad = \sqrt{\tfrac{3}{4\pi}} \qquad z/r \\
p_x \quad &= y_{11} \quad = \tfrac{1}{\sqrt{2}}(Y_1^1 - Y_{-1}^1) = \sqrt{\tfrac{3}{4\pi}} \qquad x/r \\
d_{xy} \quad &= y_{2-2} = \tfrac{i}{\sqrt{2}}(Y_2^2 - Y_{-2}^2) = \sqrt{\tfrac{15}{4\pi}} \qquad xy/r^2 \\
d_{yz} \quad &= y_{2-1} = \tfrac{i}{\sqrt{2}}(Y_1^2 + Y_{-1}^2) = \sqrt{\tfrac{15}{4\pi}} \qquad yz/r^2 \\
d_{3z^2-r^2} \quad &= y_{20} \quad = Y_2^0 \qquad\qquad = \sqrt{\tfrac{15}{4\pi}}\tfrac{1}{2\sqrt{3}}\,(3z^2 - r^2)/r^2 \\
d_{xz} \quad &= y_{21} \quad = \tfrac{1}{\sqrt{2}}(Y_1^2 - Y_{-1}^2) = \sqrt{\tfrac{15}{4\pi}} \qquad xz/r^2 \\
d_{x^2-y^2} \quad &= y_{22} \quad = \tfrac{1}{\sqrt{2}}(Y_2^2 + Y_{-2}^2) = \sqrt{\tfrac{15}{4\pi}}\tfrac{1}{2} \qquad (x^2 - y^2)/r^2
\end{aligned}
$$

B.3 Slater-Koster integrals

The interatomic Slater-Koster two-center integrals are defined as

$$E_{lm,l'm'} = \int d\boldsymbol{r}\, \overline{\psi}_{lm}(\boldsymbol{r}-\boldsymbol{d}) V(\boldsymbol{r}-\boldsymbol{d}) \psi_{l'm'}(\boldsymbol{r}).$$

They can be expressed as a function of radial integrals $V_{ll'\alpha}$, which scale with the distance d roughly as $d^{-(l+l'+1)}$ [10], and direction cosines, defined as

$$l = \boldsymbol{d}\cdot\hat{x}/d, \quad m = \boldsymbol{d}\cdot\hat{y}/d, \quad n = \boldsymbol{d}\cdot\hat{z}/d.$$

The Slater-Koster integrals for s-, p-, and d-orbitals [10] are listed below.

$E_{s,s}$	=	$V_{ss\sigma}$		
$E_{s,x}$	=	$lV_{sp\sigma}$		
$E_{x,x}$	=	$l^2V_{pp\sigma}$	$+(1-l^2)V_{pp\pi}$	
$E_{x,y}$	=	$lmV_{pp\sigma}$	$-lmV_{pp\pi}$	
$E_{x,z}$	=	$lnV_{pp\sigma}$	$-lnV_{pp\pi}$	
$E_{s,xy}$	=	$\sqrt{3}lmV_{sd\sigma}$		
E_{s,x^2-y^2}	=	$\frac{1}{2}\sqrt{3}(l^2-m^2)V_{sd\sigma}$		
$E_{s,3z^2-r^2}$	=	$[n^2-\frac{1}{2}(l^2+m^2)]V_{sd\sigma}$		
$E_{x,xy}$	=	$\sqrt{3}l^2mV_{pd\sigma}$	$+m(1-2l^2)V_{pd\pi}$	
$E_{x,yz}$	=	$\sqrt{3}lmnV_{pd\sigma}$	$-2lmnV_{pd\pi}$	
$E_{x,zx}$	=	$\sqrt{3}l^2nV_{pd\sigma}$	$+n(1-2l^2)V_{pd\pi}$	
E_{x,x^2-y^2}	=	$\frac{\sqrt{3}}{2}l[(l^2-m^2)]V_{pd\sigma}$	$+l(1-l^2+m^2)V_{pd\pi}$	
E_{y,x^2-y^2}	=	$\frac{\sqrt{3}}{2}m[(l^2-m^2)]V_{pd\sigma}$	$-m(1+l^2-m^2)V_{pd\pi}$	
E_{z,x^2-y^2}	=	$\frac{\sqrt{3}}{2}n[(l^2-m^2)]V_{pd\sigma}$	$-n(l^2-m^2)V_{pd\pi}$	
$E_{x,3z^2-r^2}$	=	$l[n^2-\frac{1}{2}(l^2+m^2)]V_{pd\sigma}$	$-\sqrt{3}ln^2V_{pd\pi}$	
$E_{y,3z^2-r^2}$	=	$m[n^2-\frac{1}{2}(l^2+m^2)]V_{pd\sigma}$	$-\sqrt{3}mn^2V_{pd\pi}$	
$E_{z,3z^2-r^2}$	=	$n[n^2-\frac{1}{2}(l^2+m^2)]V_{pd\sigma}$	$+\sqrt{3}n(l^2+m^2)V_{pd\pi}$	
$E_{xy,xy}$	=	$3l^2m^2V_{dd\sigma}$	$+(l^2+m^2-4l^2m^2)V_{dd\pi}$	$+(n^2+l^2m^2)V_{dd\delta}$
$E_{xy,yz}$	=	$3lm^2nV_{dd\sigma}$	$+ln(1-4m^2)V_{dd\pi}$	$+ln(m^2-1)V_{dd\delta}$
$E_{xy,zx}$	=	$3l^2mnV_{dd\sigma}$	$+mn(1-4l^2)V_{dd\pi}$	$+mn(l^2-1)V_{dd\delta}$
E_{xy,x^2-y^2}	=	$\frac{3}{2}lm(l^2-m^2)V_{dd\sigma}$	$2lm(m^2-l^2)V_{dd\pi}$	$\frac{1}{2}lm(l^2-m^2)V_{dd\delta}$
E_{yz,x^2-y^2}	=	$\frac{3}{2}mn(l^2-m^2)V_{dd\sigma}$	$-mn[1+2(l^2-m^2)]V_{dd\pi}$	$+mn[1+\frac{1}{2}(l^2-m^2)]V_{dd\delta}$
E_{zx,x^2-y^2}	=	$\frac{3}{2}nl(l^2-m^2)V_{dd\sigma}$	$+nl[1-2(l^2-m^2)]V_{dd\pi}$	$-nl[1-\frac{1}{2}(l^2-m^2)]V_{dd\delta}$
$E_{xy,3z^2-r^2}$	=	$\sqrt{3}lm[n^2-\frac{1}{2}(l^2+m^2)]V_{dd\sigma}$	$-2\sqrt{3}lmn^2V_{dd\pi}$	$\frac{\sqrt{3}}{2}lm(1+n^2)V_{dd\delta}$
$E_{yz,3z^2-r^2}$	=	$\sqrt{3}mn[n^2-\frac{1}{2}(l^2+m^2)]V_{dd\sigma}$	$+\sqrt{3}mn(l^2+m^2-n^2)V_{dd\pi}$	$-\frac{\sqrt{3}}{2}mn(l^2+m^2)V_{dd\delta}$
$E_{zx,3z^2-r^2}$	=	$\sqrt{3}ln[n^2-\frac{1}{2}(l^2+m^2)]V_{dd\sigma}$	$+\sqrt{3}ln(l^2+m^2-n^2)V_{dd\pi}$	$-\frac{\sqrt{3}}{2}ln(l^2+m^2)V_{dd\delta}$
$E_{x^2-y^2,x^2-y^2}$	=	$\frac{3}{4}(l^2-m^2)^2V_{dd\sigma}$	$+[l^2+m^2-(l^2-m^2)^2]V_{dd\pi}$	$+[n^2+\frac{1}{4}(l^2-m^2)^2]V_{dd\delta}$
$E_{x^2-y^2,3z^2-r^2}$	=	$\frac{\sqrt{3}}{2}(l^2-m^2)[n^2-\frac{1}{2}(l^2+m^2)]V_{dd\sigma}$	$+\sqrt{3}n^2(m^2-l^2)V_{dd\pi}$	$+\frac{1}{4}\sqrt{3}(1+n^2)(l^2-m^2)V_{dd\delta}$
$E_{3z^2-r^2,3z^2-r^2}$	=	$[n^2-\frac{1}{2}(l^2+m^2)]^2V_{dd\sigma}$	$+3n^2(l^2+m^2)V_{dd\pi}$	$\frac{3}{4}(l^2+m^2)^2V_{dd\delta}$

References

[1] E. Pavarini, E. Koch, A. Lichtenstein, D. Vollhardt (eds.)
The LDA+DMFT approach to strongly correlated materials,
Reihe Modeling and Simulation, Vol. 1 (Forschungszentrum Jülich, 2011)
`http://www.cond-mat.de/events/correl11`

[2] E. Pavarini, S. Biermann, A. Poteryaev, A.I. Lichtenstein, A. Georges, O.K. Andersen, Phys. Rev. Lett. **92**, 176403 (2004)
E. Pavarini A. Yamasaki, J. Nuss and O.K. Andersen, New J. Phys. **7**, 188 (2005)

[3] J. Kunes: *Wannier functions and construction of model Hamiltonians*, in [1]

[4] E. Pavarini: *The LDA+DMFT Approach*, in [1]

[5] M.S. Dresselhaus, G. Dresselhaus, A. Jorio:
Group Theory: Application to the Physics of Condensed Matter
(Springer, Berlin Heidelberg, 2008)

[6] M. Tinkham: *Group Theory and Quantum Mechanics* (McGraw-Hill, 1964)

[7] E. Pavarini, E. Koch, and A.I. Lichtenstein, Phys. Rev. Lett. **101**, 266405 (2008)

[8] J. Kanamori, J. Appl. Phys. **31**, S14 (1960)

[9] E. Pavarini and E. Koch, Phys. Rev. Lett. **104**, 086402 (2010)
A. Flesch, G. Zhang, E. Koch, and E. Pavarini, Phys. Rev. B **85**, 035124 (2012)

[10] W.A. Harrison: *Electronic Structure and The Properties of Solids* (Dover, 1989)